Climate Dynamics (2020) 55:449–470
https://doi.org/10.1007/s00382-020-05276-5

Interannual variability of rainfall in the Guinean Coast region and its links with sea surface temperature changes over the twentieth century for the different seasons

Koffi Worou[1] · Hugues Goosse[1] · Thierry Fichefet[1] · Françoise Guichard[2] · Moussa Diakhate[3]

Received: 6 June 2019 / Accepted: 25 April 2020 / Published online: 23 May 2020

Abstract
The summer Guinean Coast (GC) rainfall (GCR) displays a strong variability on different timescales that are driven by Sea Surface Temperature (SST) variations and amplified by land–atmosphere processes. However, the relationships between the GCR and SST modes of variability in the pre-monsoon (March–May, MAM), post-monsoon (October–November, ON) and Harmattan (December–February, DJF) seasons are not well known nor understood. Using observational dataset covering the twentieth century, we extend the conclusion obtained in previous studies that mainly analyzed the summer period (June–September, JJAS) by considering changes in SST-rainfall linkages throughout the year. We show that, in boreal winter, SST interannual variability in the tropical basins are anticorrelated with the GCR. The South Atlantic Ocean Dipole (SAOD) and the Atlantic Niño (ATL3) appear, however, as major drivers of the pre-monsoon and monsoon GCR. In MAM, both modes are in opposite phases with the GCR. Below normal SST in the tropical South Atlantic in MAM leads to a surface divergence south of the equator, and the resulting southerlies bring moist air into coastal Guinea, increasing rainfall. During JJAS, ATL3 and SAOD are in phase with the GCR. During ON, the eastern Mediterranean Sea anomalous warming strengthens the Saharan Heat Low, whose extension in the tropical North Atlantic enhances the low-level westerly Jet. This jet transports moisture into GC. The stationarity of the correlations between the GCR and SST indices has also been assessed, and the strongest and most stationary links are obtained during the monsoon season.

Keywords Guinea Coast · Rainfall · Monsoon · Teleconnection · Variability · Stationarity

1 Introduction

In mid-2019, the estimated western African population was about 391,440,000 (United Nations Department of Economic and Social Affairs/Population Division 2019), which is more than five times the population recorded in the mid-1950s. This rapid growth of population causes an important pressure on water availability in the region. Agriculture, livestock and fishing are the lungs of the West African economy, which makes the West African population vulnerable to any change in the rainfall regime. Over the twentieth century, the boreal summer SST variability in the eastern equatorial Atlantic has strongly impacted the GCR which is the main focus of this study. The covariability between ATL3 and GCR has been shown to be stationary (Diatta and Fink 2014). On the other hand, it has been shown that the relation between the rainfall in the coastal regions and the Sahel is not stationary, due to changes in the connection between the tropical Atlantic and Pacific

Electronic supplementary material The online version of this article (https://doi.org/10.1007/s00382-020-05276-5) contains supplementary material, which is available to authorized users.

✉ Koffi Worou
koffi.worou@uclouvain.be

[1] Georges Lemaître Centre for Earth and Climate Research (TECLIM), Earth and Life Institute (ELI), Université catholique de Louvain (UCLouvain), Louvain-la-Neuve, Belgium

[2] Centre National de Recherches Météorologiques, Toulouse, France

[3] École Supérieure des Sciences et Techniques de l'Ingénieur, Université Amadou Mahtar Mbow, Dakar, Senegal

(Losada et al. 2012). The vulnerability of the Sahelian area due to the strong multidecadal variability of its rainfall and the associated social-economic consequences prompted studies that aim to identify the drivers of such variability. Indeed, this area suffered from a long drought between the 1970s and 1980s, after wet conditions in the 1950s and 1960s (Hulme 1992). As briefly summarized below, our current knowledge about rainfall variability over West Africa comes from studies which focused on the Sahel. Part of the changes in the rainfall regime in this region has been attributed to different forcings, in particular the remote influence of regional and world oceans known as teleconnections, through their influence on atmospheric circulation and moisture content (Losada et al. 2009; Fontaine et al. 2009; Janicot et al. 2011; Mohino et al. 2011a; Rodríguez-Fonseca et al. 2011, 2015; Rowell 2013; Villamayor et al. 2018).

On interannual timescales, the observed summer rainfall fluctuations in the Sahel are driven by SST changes at the global scale (Folland et al. 1986; Giannini 2003), with a competition between tropical and extratropical oceanic basins. The remote effects of the different oceanic areas have been drawn out in many studies.

It has been demonstrated that the Mediterranean Sea plays an important role in modulating the rainfall fluctuation in the Sahel on interannual timescales. Years of positive summer Mediterranean SST anomalies are associated with positive summer rainfall anomalies in the Sahel and inversely (Rowell 2003). In observational climate data, there is a symmetric interrelation between warm and cold situations of the Mediterranean Sea and their respectively associated higher and lower than average rainfall in Sahel. However, sensitivity experiments conducted with Atmospheric Ocean General Circulation Models (AOGCMs) show only an increased Sahelian rainfall associated with positive SST anomalies of the eastern Mediterranean basin (Fontaine et al. 2009). In addition, it has been demonstrated that the Mediterranean SST changes affect the daily moderate, heavy and extreme rainfall in the Sahel (Diakhaté et al. 2019). Other recent sensitivity experiments have shown that, on the one hand, among the worldwide oceans, the Mediterranean basin is the main driver of the recent wet conditions over the Sahel in the boreal summer. On the other hand, this basin should be determinant for the future Sahelian rainfall (Park et al. 2016). All those studies agree that above normal SST conditions in the Mediterranean Sea give rise to moist air over the basin which is then advected southward into the Sahel. This escalates the low-level convergence in Sahel and increases rainfall over the area, together with various positive feedback processes (Jung et al. 2006). It has also been shown that the western Mediterranean SST changes drive rainfall variations in the Guinean Coast via an enhancement of deep convection in the eastern equatorial Atlantic (Fontaine et al. 2009).

In the North Atlantic, numerous studies pointed out the major influence of the Atlantic Multidecadal Oscillation (AMO) on the seasonal, interannual and decadal/multidecadal rainfall variability in West Africa, especially in the Sahel. The AMO-Sahelian rainfall link has been shown to be very strong on decadal-multidecadal timescales (Berntell et al. 2018). During AMO positive phases, the strengthening of the shallow meridional circulation (SMC) associated with the Saharan Heat Low (SHL) allows a southerly moisture flux which increases spring rainfall in the Sahel (Martin and Thorncroft 2014). In summer, in addition to a strengthening of the SMC, positive AMO phases induce above normal SST conditions in the Mediterranean Sea which in turn are favorable to more moisture convergence in the Sahel leading to more rainfall. Thus, AMO positive (negative) phases are associated with positive (negative) rainfall anomalies in the Sahel (Knight et al. 2006; Rodríguez-Fonseca et al. 2011, 2015; Martin and Thorncroft 2014; Schubert et al. 2016).

The leading mode of covariability between the West African rainfall and the tropical Atlantic SST links the summer rainfall in the Gulf of Guinea with SST changes in the eastern equatorial Atlantic (Polo et al. 2008). These SST changes associated with this mode are referred to as the Atlantic equatorial mode (AEM) or Atlantic Niño (ATL3). The Atlantic Niño also appears as the leading SST mode of variability in the tropical Atlantic (Dommenget and Latif 2000, 2002; Keenlyside and Latif 2007; García-Serrano et al. 2008; Richter et al. 2012; Mohino and Losada 2015). Basically, warm phases of the sea surface temperature anomalies (SSTAs) in the ATL3 area lead to a dipole pattern of rainfall in West Africa, with positive rainfall anomalies along the Coast of Guinea and negative rainfall anomalies in Sahel. The linkages between the Atlantic Niño and the West African rainfall are not linear, as underlined by model sensitivity experiments. The positive and negative phases of the Atlantic equatorial mode induce, indeed, changes in rainfall of different magnitudes (Losada et al. 2010). Over the twentieth century, the summer ATL3–GCR relationship appears stationary (Diatta and Fink 2014).

In the South Atlantic Ocean (SAO), a dipole defined as the difference between SSTAs in the North East Pole (NEP, an area in the ATL3 domain) and the South West Pole (SWP, an area along the Argentina-Uruguay-Brazil) is termed the South Atlantic Ocean Dipole (SAOD). On interannual timescales positive phases of the SAOD are strongly related to positive summer rainfall anomalies in the Guinean Coast and inversely (Nnamchi and Li 2011). The connection of this coupled ocean–atmosphere phenomenon with the Guinean Coast operates via the Lindzen–Nigam process (Lindzen and Nigam 1987): during positive phases of the SAOD, large subsidence and divergence occur in the SWP, and are related to strong convergence and upward motion of humid air over the NEP. This leads to a flux of moisture from the Gulf of

Guinea and equatorial Atlantic into areas in the Coast of Guinea. Note that the SAOD positive phases are associated with a reduction of the Indian monsoon rainfall (Kucharski and Joshi 2017).

Remote effects of the Pacific Ocean have been linked with changes of the Sahelian rainfall in boreal summer: in general, above normal SST anomalies in the central and eastern Pacific or SST anomaly gradient from the western Pacific to the eastern Indian Ocean are associated with negative rainfall anomalies in the Sahel (Rowell 2001). The connection between the Pacific Ocean and West Africa under those particular SST conditions operate via the propagation of Kelvin (eastward) and Rossby (westward) waves. This enhances subsidence over the Sahel region. In addition, since the 1970s, from May to September, the dry belt induced by the positive SSTAs in the Pacific Ocean migrates progressively from the Guinean Coast to the Sahel (Mohino et al. 2011b). In the northern Pacific, an opposite phase relationship has been established between the Interdecadal Pacific Oscillation and Sahelian rainfall in boreal summer on decadal to multidecadal timescales (Mohino et al. 2011a).

The Indian Ocean exhibits an opposite phase relationship with the Sahelian rainfall on decadal timescales (Rowell 2001; Bader and Latif 2003). Indeed, the Sahelian wet conditions in the 1950s–60s are linked with negative SST anomalies in the Indian Ocean, while the warming trend of this latter in the 1970s could be associated with the severe 1970s Sahelian long drought.

On smaller, regional scale, some features of the atmospheric circulation also play important roles in the rainfall genesis over West Africa. One key feature is the presence of different veins of wind which combine with the low-level moisture flow, such as the mid-level African Esterly Jet (AEJ) at 650 hPa (Cook 1999; Hsieh and Cook 2005) and the high-level Tropical Easterly Jet (TEJ, 200 hPa). Their positions, intensities as well as the activity of waves induced by e.g. instabilities in their core modulate the frequency and intensity of rainfall (Thorncroft and Hoskins 1994a, b; Thorncroft and Blackburn 1999; Nicholson and Grist 2003; Gu and Adler 2004; Nicholson 2009, 2013; Sylla et al. 2011; Kebe et al. 2016). The African Easterly Jet takes its origin in the meridional temperature gradient between the Saharan desert and the Atlantic Ocean, while the Tropical Easterly Jet results from an intense north–south temperature gradient between the Himalayan Plateau and the Indian Ocean. Additionally, the presence of the Saharan Heat Low (SHL) and its associated Shallow Meridional Circulation (SMC) have been identified as a major driver of the Sahelian rainfall (Hagos and Zhang 2009; Lavaysse et al. 2015; Shekhar and Boos 2017). The Saharan Heat Low forms as a result of high temperature over the Saharan desert. Its presence induces a shallow meridional circulation: northward winds from the Sahel converge at the core of the SHL, leading to an ascent followed by a divergence at 700 hPa and a southward displacement of the wind at that level. Those studies update the former view of the West African rainfall variability which has been thought to be controlled by the seasonal cycle of the Intertropical Convergence Zone (ITCZ), where at the surface, hot and dry northeasterly Harmattan winds blow over the Sahara and meet cold and moist southwesterly winds that originate from the Atlantic Ocean. Ascending motion of air then leads to cloud systems and the associated rainfall (Germain 1968; Dettwiller 1965; Walker 1957; Hamilton et al. 1945; Sansom 1965). In addition, over the West African continent, the term ITCZ is confusing and sometimes, the Intertropical Discontinuity and Intertropical Front are used instead, and correspond to the place where dry northeasterlies meet southwerterlies (monsoon flow).

The different studies presented above attest of the great progress accomplished in the identification and understanding of the role of the oceanic forcing and other synoptic systems on rainfall variability in West Africa. Most of those works are, however, much focused on the Sahelian area and the boreal summer, which account for about 85% of the Sahelian annual rainfall. The number of studies devoted to the Guinean Coast is much smaller, and the dynamics over this region is quite distinct. Indeed, spring rainfall in the Guinean Coast is controlled by the development of a cold tongue in the equatorial Atlantic (Nguyen et al. 2011; Meynadier et al. 2015); this cold tongue can also influence the rainfall onset of the Sahel without being the main driver (Caniaux et al. 2011; Steinig et al. 2018). Moreover, those studies investigated the SST-rainfall relationship in the Guinean Coast during the summer period. However, 40% of the annual rainfall falls in this area from October to May (against 15% in the Sahel). This motivates the present study which analyzes the oceanic influence on the interannual Guinean Coast rainfall for all the seasons over the twentieth century and the last decades. The stationarity of the relationships are then analyzed, and the major SST indices are pointed out.

2 Data and methods

The present study focuses on the 1901–2016 period. The monthly rainfall product comes from CRU TS v4.01 (Climate Research Unit Time Series). It is a gridded rainfall data which covers only lands at a resolution of 0.5° and which spans from 1901 to 2016 (Harris et al. 2013; University of East Anglia Climatic Research Unit et al. 2017). The monthly SST data selected for the analyses are derived from the version 1 of the Hadley Centre Global Sea Ice and Sea Surface Temperature (HadISST1) (Rayner 2003), which extends from 1870 to 2017 at a resolution of 1° latitude by 1° longitude.

Four different seasons have been considered: the Harmattan season or DJF (December, January, February), the pre-monsoon season or MAM (March, April, May) , the monsoon season or JJAS (June, July, August, September) and the post-monsoon season or ON (October, November). The definition of DJF and MAM are consistent with Zhang et al. (2006), Abiodun et al. (2012) and Senghor et al. (2017), while JJAS is consistent with Rodríguez-Fonseca et al. (2011) and Diatta and Fink (2014).

Monthly SST and rainfall anomalies are first computed from the linearly detrended SST and rainfall data. Then, monthly SST and rainfall indices are computed as area-averaged anomalies over different regions, based on the literature and defined in Table 1. Particularly, for West Africa, two rainfall indices are computed for areas lying between 5° N and 10°N and 20° W–10° E. This classic delimitation is based, for example, on the center of action of the second mode of summer rainfall variability in West Africa. The leading mode has its main center of action on the Sahel. Those modes are obtained by applying an Empirical Orthogonal Functions (EOFs) analysis (Monahan et al. 2009; Dommenget and Latif 2002; Wilks 2011) on rainfall anomalies over West Africa. For the North Pacific SST index (NPAC), the monthly SST indices are defined as the standardized expansion coefficients of the leading EOF mode of variability of the northern Pacific Ocean. Besides, seasonal SST and rainfall indices are derived from the monthly indices by their averages over months defining each season.

In addition, as much of the rainfall variability of Guinea Coast occurs on interannual timescales (Diatta and Fink 2014), the present study focuses on that time period. This is achieved by first applying a low pass Lanczos filter (Duchon 1979) to all the time series of each seasonal index, with a cutoff of 8 years. The main results do not change if a cutoff

Table 1 Summary of the various indices computed for the analyses

	Index definition	Lat min	Lat max	Lon min	Lon max	Method
GC	Guinean Coast	5	10	− 20	10	Area average
SH	Sahel	10	20	− 20	10	“”
NATL	North Atlantic SST	0	70	− 75	− 10	“”
MED	Mediterranean Sea	30	40	− 5	35	“”
MEDE	Eastern Mediterranean Sea	30	40	20	35	“”
MEDW	Western Mediterranean Sea	30	40	− 5	20	“”
NAT	North Atlantic Tropical SST	5	20	− 40	− 20	“”
SAT	South Atlantic Tropical SST	− 20	− 5	− 15	5	“”
TASI	Tropical Atlantic SST meridional gradient	−	−	−	−	*NAT–SAT*
TNA	Tropical Northern Atlantic	5	25	− 55	− 15	Area average
TSA	Tropical Southern Atlantic	− 20	0	− 30	10	“”
ATL3	Atlantic Niño	− 3	3	− 20	0	“”
NEP	North East Pole	− 15	0	− 20	10	“”
SWP	South West Pole	− 40	− 25	− 40	− 10	“”
SAOD	South Atlantic Ocean Dipole	–	–	–	–	NEP–SWP
NINO3	Niño3	− 5	5	− 150	− 90	Area average
NINO34	Niño3.4	− 5	5	− 170	− 120	“”
NINO4	Niño4	− 5	5	160	− 150	“”
TA	Region A	− 10	10	165	− 140	“”
TB	Region B	− 15	5	− 110	− 70	“”
TC	Region C	− 10	20	125	145	“”
EMI	El-Niño Modoki	–	–	–	–	1.0 · TA–0.5 · TB–0.5 · TC
IEMI	Improved El-Niño Modoki	–	–	–	–	3.0 · TA–2.0 · TB–1.0 · TC
NPAC	North Pacific	20	70	120	− 105	EOF 1
WTIO	West Tropical Indian Ocean SST	− 10	10	50	70	“”
SETIO	Southeastern Tropical Indian Ocean SST	− 10	0	90	110	“”
DMI	Dipole Mode (Indian Ocean)	−	−	−	−	WETIO–SETIO
CINDO	Center of Indian Ocean	− 25	10	55	95	Area average
IPWP	Indo-Pacific Warm Pool	− 25	25	40	− 140	“”

Results for indices which names are tilted are not shown in these analyses. Latitudes and longitudes are in °. Some indices are defined by the following link: https://stateoftheocean.osmc.noaa.gov/sur/. Additionally, indices defining El-Niño Modoki follow Li et al. (2010)

of 10 years is chosen. This provides low frequency changes which are secondly removed from the initial seasonal index. The remaining time series are here considered as the high-frequency interannual timescale index. For the Guinean Coast rainfall indices, filtered and unfiltered time series are also compared. Finally, the stationarity of the covariability between the rainfall and oceanic modes of variability has been assessed by performing a running correlation, with different lengths of the sliding window and different starting years.

The significance level of the Pearson correlation coefficients calculated in this work has been set to 95% confidence level according to a Fisher-test. Following Taubenheim (1969), the significance of a linear correlation r between two time series $x(t)$ and $y(t)$ of size N can be assessed by computing a critical value of the F parameter defined as:

$$F_{cri} = \frac{r^2}{1 - r^2}(N - 2) \tag{1}$$

where $N - 2$ is the standard degree of freedom ($SDOF$). To take into account autocorrelation in the time series, an effective degree of freedom ($EDOF$) is computed (Taubenheim 1974; Fink and Speth 1997):

$$EDOF = 1 + \frac{N}{1 + 2\sum_{l=1}^{N-1} \frac{N-l}{N} K_x(l)K_y(l)} \tag{2}$$

where $K_x(l)$ and $K_y(l)$ are the autocorrelation functions at lag l. Then, from the F-distribution with $d_1 = 1$ and $d_2 = SDOF$ or $d_2 = EDOF$ degrees of freedom (d_1 and d_2 are the degrees of freedom of the Fisher's law), the probability (p_{value}) to exceed the F_{cri} is computed. Therefore, r values are significant if $p_{value} \leq 0.05$. The results of the two tests are shown to highlight differences if our series are autocorrelated.

Finally, we used ERA-20C (Poli et al. 2016), a reanalysis product from the European Centre for Medium-Range Weather Forecasts to highlight the physical key mechanisms associated to the strongest connections that are obtained. It is available for the 1900–2010 period. For each season, SST index of the main oceanic mode of variability is calculated from the reanalysis data. Then, this index is standardized and regressed onto various atmospheric fields to underline the mechanisms by which the oceanic mode influences the rainfall in the coastal Guinea. Similarly, circulation fields associated with each seasonal rainfall index is available in the Online Resource. Although we have selected standard observational datasets used in many applications (e.g. Rowell 2003; Gómara et al. 2017 for HADISST data, and Diatta and Fink 2014; Bamba et al. 2015; Salih et al. 2018; Okoro et al. 2019 for CRU data), including in West Africa, their validation is beyond the scope of this work. One must keep in mind that some limitations of our results may come from uncertainties in these datasets (as well as biases in the reanalysis products) which are the object of several ongoing studies (e.g. Hirahara et al. 2014; Huang et al. 2016).

3 West Africa: mean climate, annual cycle and variability

The West African rainfall is dominated by a monsoon system which is responsible for more than 58% of the annual rainfall in the Guinean Coast and 84% in the Sahel (the contribution of each season for the total annual rainfall of the Sahel and Guinean Coast can be found in Table 2). During the Harmattan season (DJF), when northeasterlies are strong over the region, weak rain falls over West Africa (Fig. 1a). More intense rainfall occurs in March in coastal areas. During the MAM season, the rainfall maximum lies between 4° N and 9° N. In June, the rainfall reaches a maximum mean of about 8 mm day^{-1} over the Guinean Coast (Fig. 1b). Then, the rainbelt moves northward in the Sahel, where the mean rainfall rate peaks to about 6 mm day^{-1} in August. At the same time, rainfall slightly decreases over the Guinean Coast. This corresponds to the "little dry season" (Adejuwon and Odekunle 2006; Froidurot and Diedhiou 2017; Fink et al. 2017). In September, the rainfall maximum moves back equatorward, which implies a second maximum over the Coast of Guinea, with a mean intensity of more than 8 mm day^{-1}. This corresponds to the highest monthly fraction of the annual rainfall in the Guinean Coast (16%, Fig. 1b). Consequently, the Guinean Coast and the Sahel rainfall annual cycles exhibit two different patterns, with respectively a bimodal and a unimodal structure (Fig. 1).

A change of the rainfall annual cycle in the Guinean Coast has been observed during the last century. Regarding the 1901–2016 period, the annual cycle is characterized by a bimodal structure, with two maxima, in June and September respectively. When focusing on the four consecutive 20-year periods prior to 1980, this bimodal annual cycle is well defined. However, after 1980, the bimodality becomes less pronounced, it even vanishes over 1981–2000, with a single maximum in August. Then it shifts to September for the 2001–2016 period (Fig. 2a). The analysis of the monthly Guinean Coast rainfall variance shows no substantial change in each month, except July, August and September (Fig. 2b). However, the rainfall variance has changed for the other months. For example, low variance is observed over the 1921–1940 period, for July, August and September. Then, it increases over 1941–1960. For the following period, the variance decreases for August and September while it continues to grow in July. In the 1981 – 2000 period, the variance decreases dramatically for July, while it slightly increases for August and September. Then, an increasing trend is observed for June, July and September in the 2001–2016 period relative to the 1981–2000. Otherwise, for

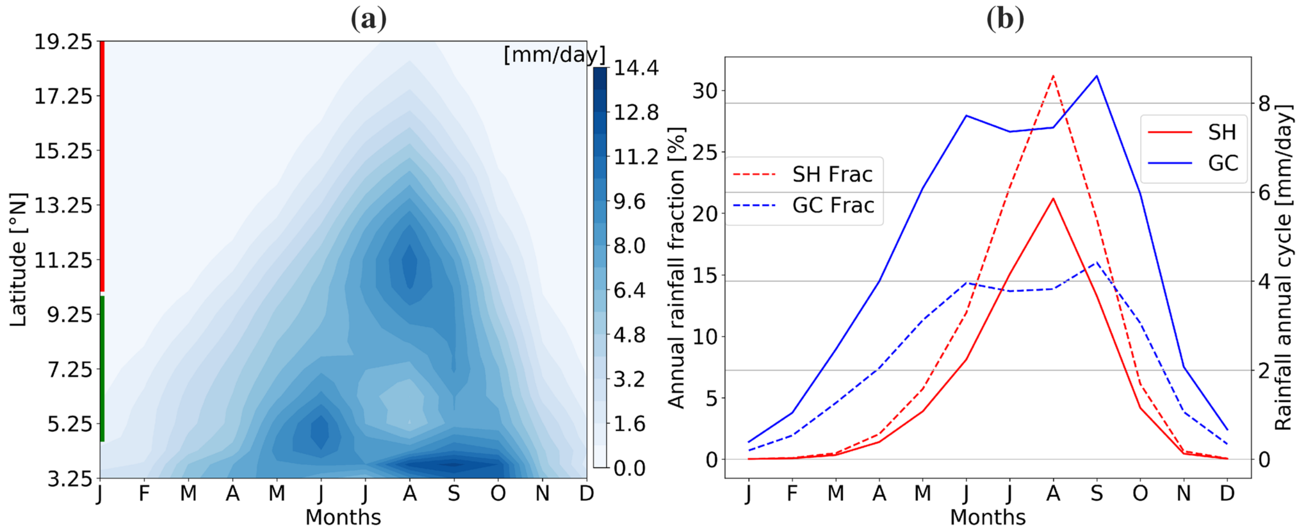

Fig. 1 **a** Time-latitude evolution of rainfall mean over 20° W and 10° E. The green and red lines delineate latitudes corresponding to the Guinean Coast and Sahel regions respectively. **b** Annual cycle of rainfall mean (full lines) and annual rainfall fraction (dotted lines) for the Guinean Coast (in blue) and the Sahel (in red). Analyses are performed for the 1901–2016 period

August, the trend is decreasing for those last two periods. These changes are reflected in the seasonal rainfall indices of the coast of Guinea (Fig. 3i–l) which will be analyzed rather than monthly rainfall indices.

Figure 3a–d shows that each Guinean Coast rainfall index exhibits a negative trend for the 1901–2016 period. This trend is more pronounced for the pre-monsoon and post-monsoon seasons, with a slope of – 0.005 and – 0.004 mm day^{-1} year^{-1} respectively. For the DJF and JJAS seasons, the value of the slope is reduced to – 0.002 mm day^{-1} year^{-1}. The maximum rainfall variance of the Guinean Coast rainfall has been obtained in the monsoon season (JJAS), with a standard deviation of 0.85 mm day^{-1}, followed by the ON, MAM and DJF seasons. The values obtained for these three seasons are 0.75, 0.5 and 0.22 mm day^{-1}, respectively. Similar results are found for the variance of the high pass filtered indices (Fig. 3e, f). This shows that much of the GC rainfall variability happens on interannual timescales. In addition, the 20-year sliding window of the standard deviation of the rainfall is illustrated in Fig. 3i–l. The variances obtained are normalized to the 1901–2016 period. Results show for DJF an increase of the rainfall variance from the 1950s to the 1970s. For MAM, the rainfall variance decreases in the first 2 decades, then it remains constant until the 1960s before increasing. From the 1970s, a decreasing variance is observed. For JJAS, a decreasing trend of the variance is observed over the 1940–2000 period. Then, it increases afterwards. ON rainfall also shows the same decreasing trend until 1975s, from which the variance remains constant. For JJAS and ON, the rainfall variance increases over the 1925–1950 period. The pronounced decrease of the rainfall variance in the Guinean Coast (particularly in the boreal summer) has coincided with a reduction of the variability of the Atlantic cold tongue (Tokinaga and Xie 2011). This is due to an enhanced warming of SST in the Atlantic cold tongue area, which has decreased the trade winds intensity and lead to a weakening of upwelling in the eastern equatorial Atlantic. Consequently, the thermocline has deepened, reducing the cold tongue and the variability of the Atlantic equatorial mode as well as the rainfall in the coastal Guinea.

Hereafter the influence of SST modes of variability on the Guinean Coast rainfall regime will be evaluated separately for the four seasons on interannual timescales. Figure 4a–d presents the spatial distribution of the mean rainfall over West Africa and its evolution through the seasons. It shows an increase of the rainfall mean from the Harmattan season (DJF) to the pre-monsoon season (MAM), mainly in the Guinean Coast. Then the rainbelt moves northward in JJAS, with the highest values of rainfall in the Guinean Highlands and Cameroon mountains. In the post-monsoon season, the maximum values are located in the Guinean Coast. Figure 4e–h shows that the core of the Guinean Coast rainfall correlation pattern (correlation between the seasonal Guinean Coast rainfall index and the West African rainfall anomalies) is located in the Guinean Coast latitudinal band in DJF and JJAS. As shown in Fig. 4a, weak rain falls in the Sahel in DJF, explaining the southward location of the correlation pattern. For JJAS, differences in the oceanic drivers of the West African rainfall could explain the main coastal core of the Guinean Coast rainfall correlation pattern. In particular, the disappearance of the West African Westerly Jet (WAWJ) in warm phases of the eastern equatorial Atlantic could reduce the zonal moisture transport onto the Sahel

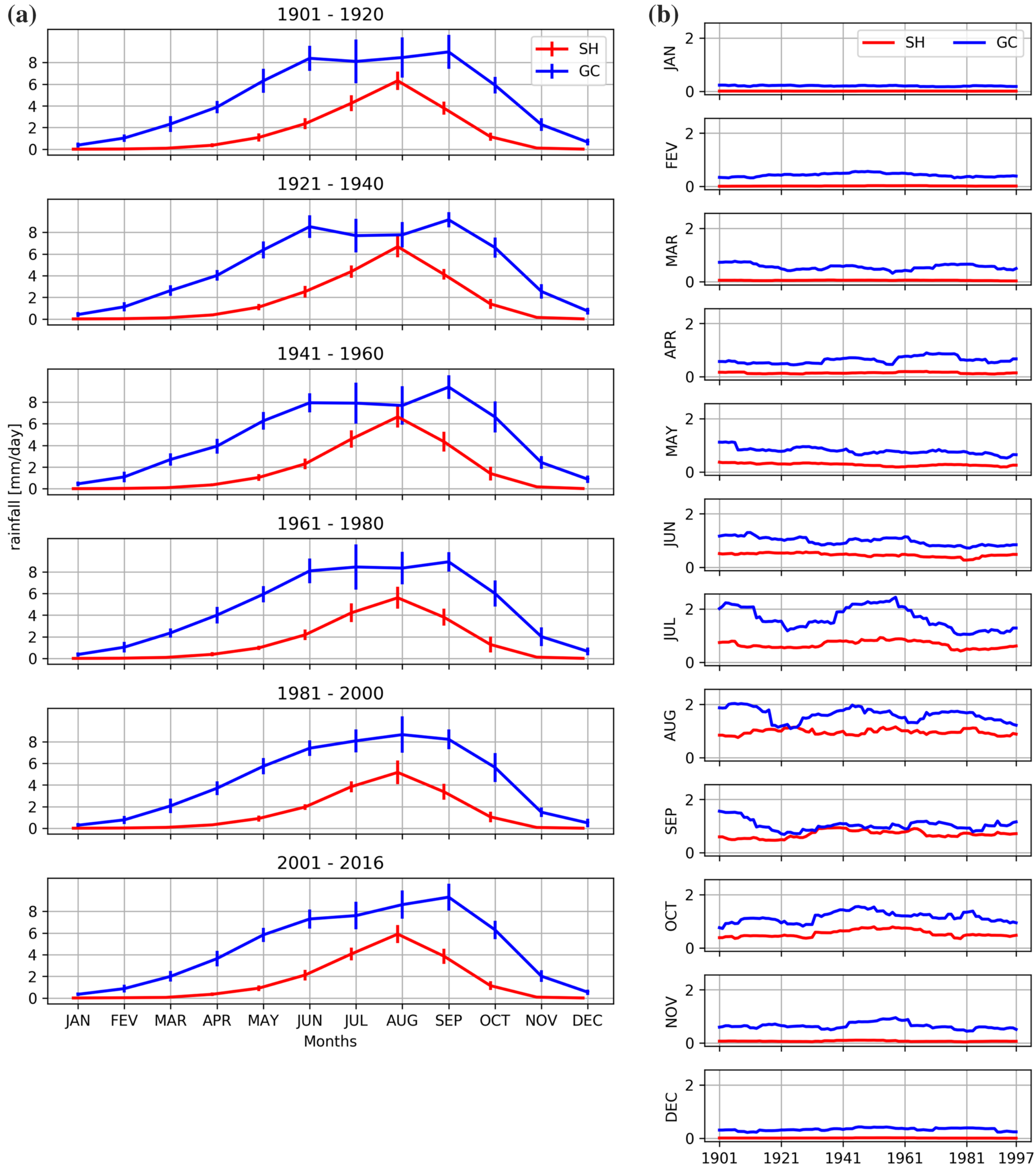

Fig. 2 **a** Annual cycle of rainfall in the coast of Guinea (in blue) and Sahel (in red) over different periods of 20 years (the last period counts 16 years). **b** Standard deviations of the mean Guinean Coast (in blue) and Sahelian (in red) rainfall over sliding 20-year periods

(Lélé and Leslie 2016). In MAM and ON, the Guinean Coast rainfall correlation pattern extends over whole West Africa. The corresponding SST patterns are displayed in Fig. 4i–l. This figure shows high correlation values over large areas during the Harmattan and monsoon seasons, while in the pre-monsoon and post-monsoon seasons, the correlation values are low, and confined in few oceanic areas. In addition, a reversal of the sign of the correlation is observed between

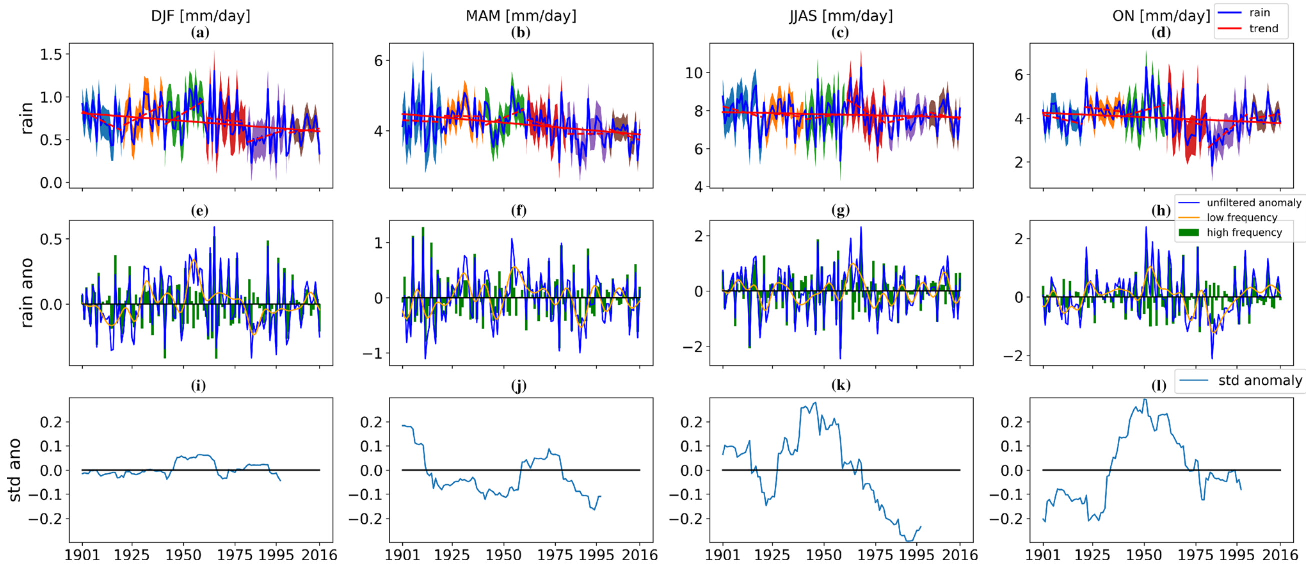

Fig. 3 **a–d** Seasonal unfiltered rainfall indices and trends for the Guinean Coast. The trend over the 1901–2016 period is indicated by the red lines. Red dashes (shades) show the trend (standard deviation) over periods of at least 20 years from 1901. **e–h** Low (orange curves) and high (green bars) frequency components of the unfiltered seasonal rainfall anomalies of the coast of Guinea (blue bars). **i–l** Anomalies of the sliding 20-year standard deviation of the seasonal high-pass Guinean Coast rainfall index relative to its full value for 1901–2016. Indices are computed for the period 1901–2016

the DJF and JJAS seasons in the tropical South Atlantic and areas in the eastern tropical Indian Ocean and Maritime Continent (oceanic area between the eastern Indian Ocean and the western tropical Pacific Ocean). Those observations show that, throughout the seasons, the interrelation between the Guinean Coast rainfall and SST changes, and needs to be evaluated separately.

4 Oceanic forcing of the Guinean Coast rainfall variability: dominant SST modes of variability and robustness of the linkages

4.1 Oceanic forcing of the Harmattan (DJF) Guinean Coast rainfall

The mean DJF rainfall in West Africa over the 1901–2016 period ranges between 0 and 3 mm day^{-1}, depending on the location (Fig. 4a). Rainfall during this season corresponds to about 4% of the annual rainfall over the Guinean Coast (Table 2). Although this value is low compared to the other seasons, the DJF Guinean Coast rainfall plays an important role, as meteorological conditions of that season are crucial for the growing of agriculture products such as coffee and cocoa (Ehounou et al. 2019a, b; Lahive et al. 2018). Studies show that this growth requires an annual rainfall between 1200 and 1500 mm (Dian 1978; Lachenaud 1987, 1991; Brou et al. 2003; Kassin et al. 2008; Köhler et al. 2010; Saj et al. 2017). Moreover, three consecutive months of dry conditions could be dramatic for the growth of cocoa, which is why it is capital to monitor and understand the drivers of DJF rainfall variability, as this season is the driest one of the year. The rainfall correlation pattern associated with the interannual Guinean Coast index has a core of positive values which principally lies between 5° N and 10° N (Fig. 4e). To determine the oceanic areas that are related to this rainfall mode, the DJF Guinean Coast rainfall index has been correlated with global SSTAs of the same season (Fig. 4i). The results show that above normal rainfall anomalies in the coast of Guinea are associated with strong negative SSTAs in the eastern tropical Pacific, eastern (western) boundaries of the tropical Indian (Pacific) Ocean. Few oceanic areas in the tropical South Atlantic and western Mediterranean Sea present negative correlations, while positive correlations are obtained in the Red Sea, eastern Mediterranean Sea, extratropical North Atlantic and tropical North Atlantic.

In a second step, the role of different SST modes of variability on the West African rainfall in DJF has been evaluated. The correlation between each SST index and the Guinean Coast rainfall for all seasons is displayed in Fig. 5. However, the discussion will be focused on the main SST modes which results are summarized in Fig. 6. Those oceanic modes have the strongest impact (highest correlation and best stationarity feature) on the Guinean Coast rainfall. In agreement with the DJF large-scale SST pattern in Fig 4i, the El-Nino (Niño3), Indo-Pacific warm pool [IPWP, defined as the oceanic area within 40° E–140° W, 25° S–25° N, where the SST is above

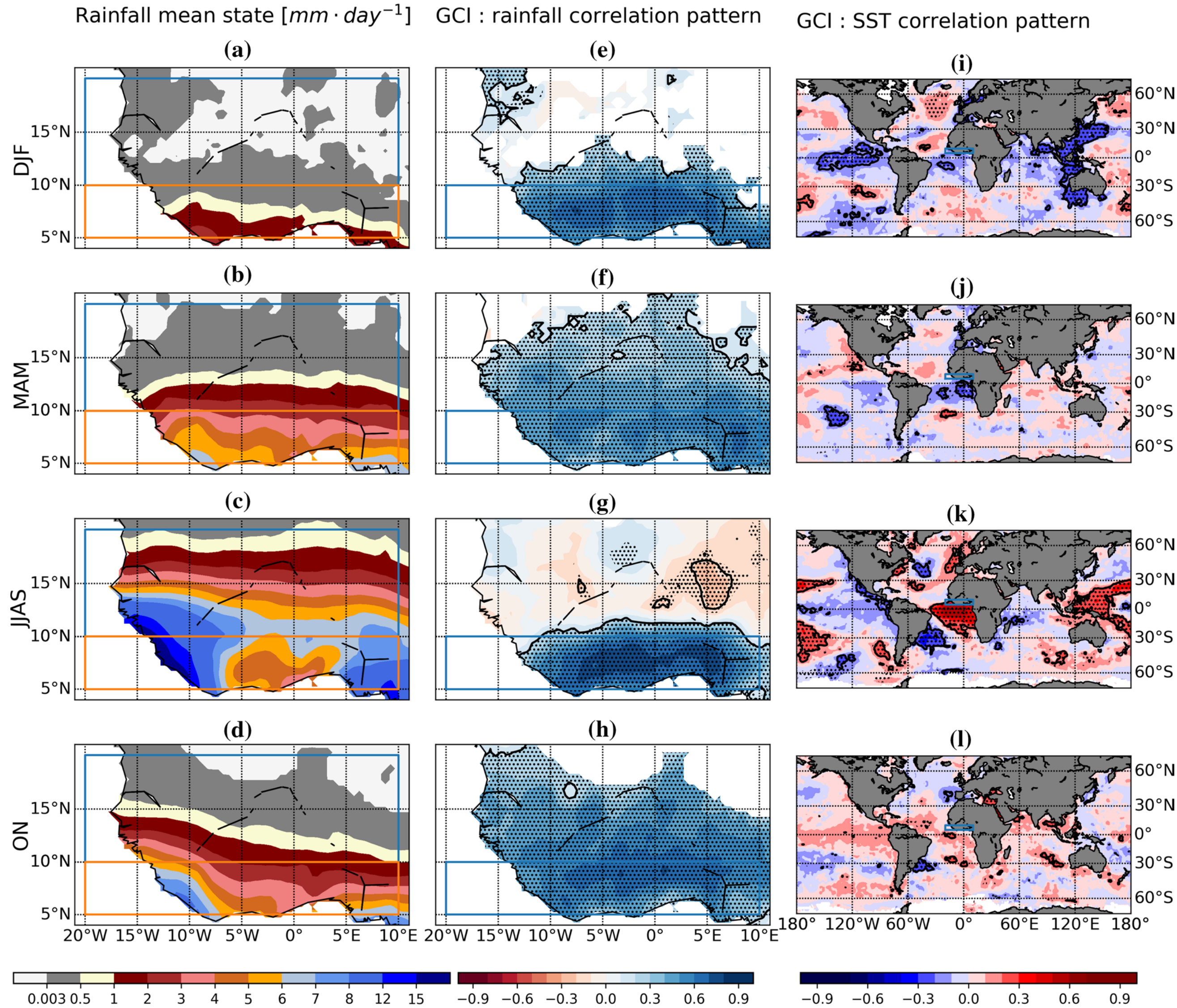

Fig. 4 **a–d** Seasonal mean of rainfall rates over West Africa. **e–h** Correlation between the high-frequency Guinean Coast rainfall index and the seasonal rainfall anomaly at each grid point. **i–l** Correlation between the high-frequency Guinean Coast rainfall index and SST anomalies for each season. Contour lines and dots in the correlation patterns represent significant values at 95% confidence level according to a F test with respectively a standard degree of freedom and the effective degree of freedom. Analysis is performed for the 1901–2016 period

Table 2 Annual rainfall fraction (in %) for each season and each area (Sahel and Guinean Coast)

	DJF	MAM	JJAS	ON
Sahel (20° W–10° E, 10°–20° N)	0.2	8.3	84.7	6.8
Guinean Coast (20° W–10° E, 5°–10° N)	3.9	23.3	57.9	14.9

Fractions are computed for the 1901–2016 period, as a seasonal cumulative mean rainfall over the cumulative annual rainfall. Those values are computed from CRU TS v4.01 rainfall data (University of East Anglia Climatic Research Unit et al. 2017)

28 °C all the year, (Weller et al. 2016; Deckker 2016)] and Atlantic Niño (ATL3) indices are negatively correlated with rainfall anomalies in the Coast of Guinea, while the eastern Mediterranean SST index shows overall positive correlations (Fig. 6a–e). The influence of the Atlantic Niño is located in the western area of the Guinean Coast, while that of IPWP is more pronounced in the northeastern boundary of Guinea Coast, as well as in the southwestern coast. Relative to the IPWP SST index, indices of El-Niño have few significant correlations with the rainfall anomalies in West Africa. As for the eastern Mediterranean SST index, the significant correlations lay between 5° W-5° E and 7°N-10° N. The spatial

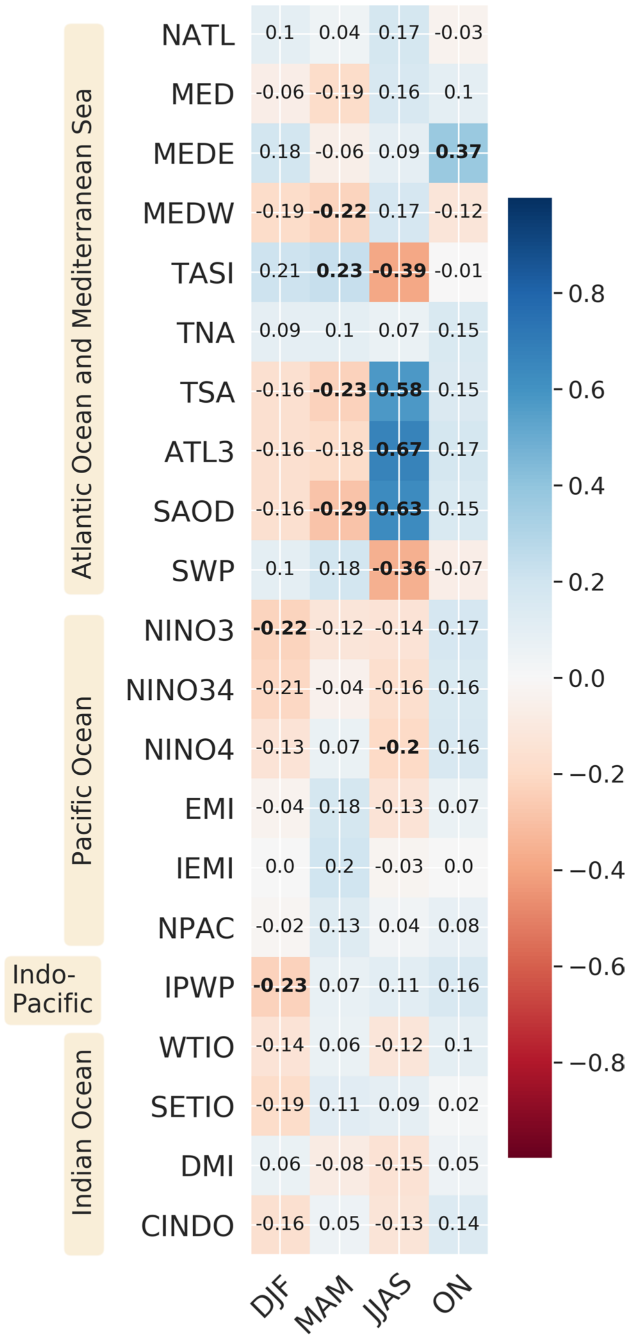

Fig. 5 Correlation between different SST indices and the Guinean Coast rainfall index for different seasons (1901–2016 period). Significant values at 95% confidence level based on a F test taking into account serial correlations are shown in bold

pattern of the West African rainfall correlation with each oceanic mode of variability is instructive. It shows the spatial rainfall differences in response to the influence of a given oceanic internal mode of variability.

Although Figs. 4i–l and 5 show the most robust linkages over the full 1901–2016 period, they could not identify the stationarity of those links nor provide any information about the periods over which the connections were the strongest. There is then a need to test the changes in the correlation according to the length of the samples as well as their starting year. The robustness of the DJF SST-rainfall relationships has been evaluated and displayed in Fig. 7a–e. For the 1901–2016 period, the IPWP index has the strongest correlation of – 0.23 with the Guinean Coast rainfall index. The correlation remains constant (the sign) and significant for samples wider than 65 years in that period, with values between – 0.4 and – 0.2. For samples which sizes are between 20 and 65 years and starting in the 1920s–1970s period, this anticorrelation strengthens, with predominant values ranging between – 0.75 and – 0.4. This highlights that the influence of the IPWP happens mainly on interannual timescales. Likewise, IPWP, ATL3 and Niño3 indices present overall similar changes of their correlation with the GCR index. In addition, the interannual indices of $NINO_3$ and IPWP are strongly coupled all the time, whereas the IPWP interannual linkage with the coastal Guinean rainfall takes place when the IPWP co-varies with the tropical South Atlantic. Consequently, the weakening of the coupling between IPWP and ATL3 before 1920s and after 1970s could explain the non-stationary correlations between the IPWP SST and GCR on interannual timescales (Fig. S14, Online Resource). This is illustrated in the Figures S6 and S7d (Online Resource): over the 1925–1970 period, the ATL3 is positively correlated with SSTAs in the tropical oceans, while over 1980–2016, the core of the ATL3 correlation pattern with SSTAs is mainly restricted to the Atlantic equatorial and southern basin. Consistently, the 1925–1970 correlation between the GCR index and SSTAs (Fig. S2i, Online Resource) shows negative values in the whole tropics, while over 1980–2016, weak coupling is found in tropical South Atlantic (Fig. S3(i), Online Resource). During the 1925–1970 period, a well pronounced negative rainfall correlation with IPWP and ATL3 extends over the Guinea Coast and north of 10° N (Figs. S4b and d, Online Resource). For 1980–2016, except in very localized small areas, weak correlations are found between rainfall anomalies in Guinea Coast and the SST indices (Figs. S5a–e, Online Resource).

Results with one single 31-year sliding window are available in Fig. 8, which illustrates the methodology of the stationarity evaluation for a particular window length. It can be seen that for the DJF season (Fig. 8a–e), the eastern Mediterranean SST and the Guinean Coast rainfall correlation is positive but hardly significant between 1930s and 1950s. For the IPWP SST index, the correlation with the Guinean Coast index is stationary from 1935s to 1985s, with values ranging between – 0.6 and – 0.4. In addition, the Niño3 mode is in opposite phases with the Guinean Coast rainfall in the 1950–1985 period (correlation between – 0.6 and – 0.2). Finally, the ATL3 mode shows negative correlations (between – 0.6 and – 0.3) in the 1940–1975 period. Note

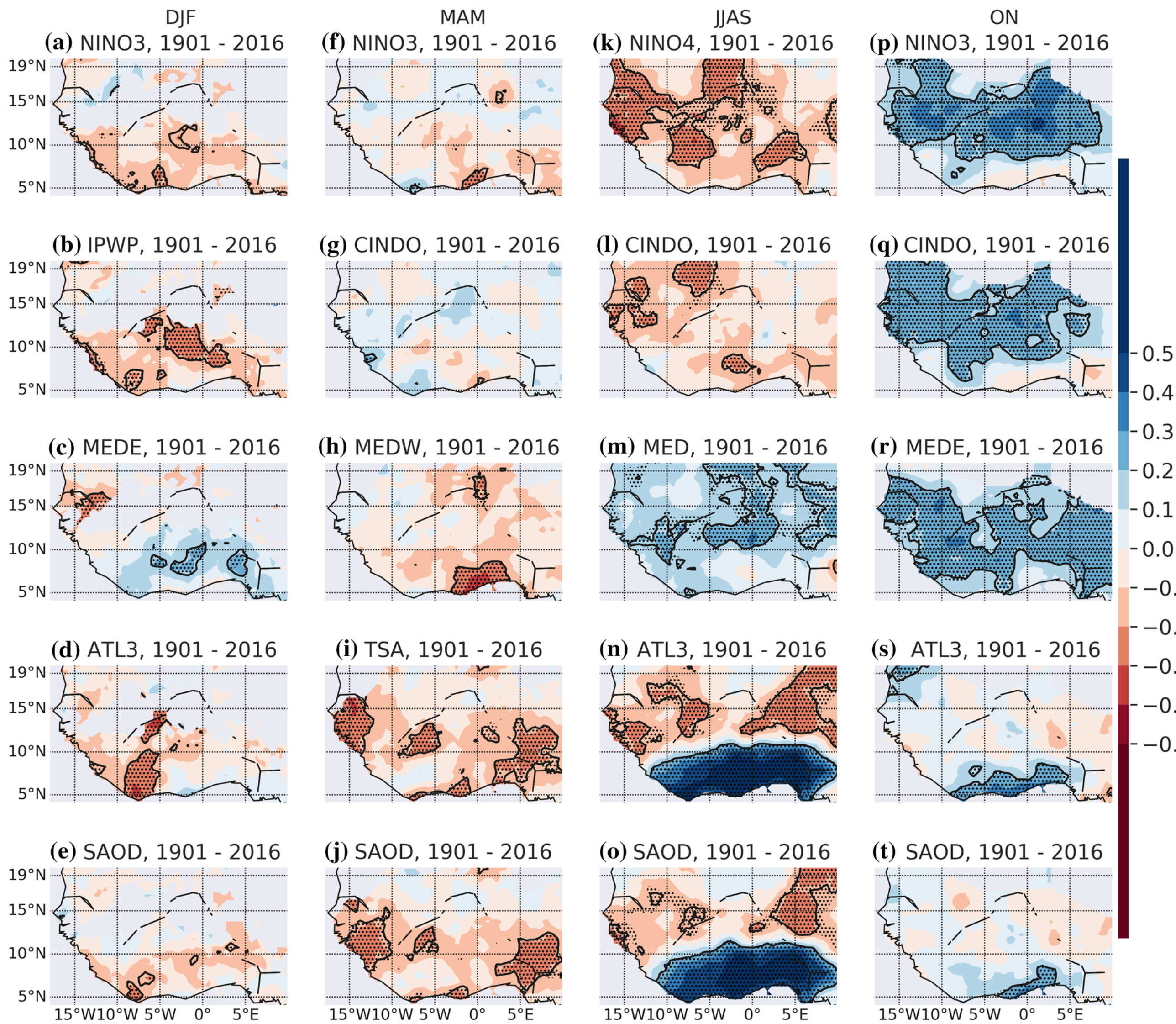

Fig. 6 Rainfall patterns associated with the main SST modes of variability for each season: **a**–**e** DJF, **f**–**j** MAM, **k**–**o** JJAS, **p**–**t** ON. Those patterns are obtained by correlating the interannual SST indices with rainfall anomalies in West Africa. Contour lines and dots indicate significant correlations at 95% confidence level according to a F test with a standard and effective degree of freedom, respectively

that the rainfall index relative to the Sahelian area exhibits a similar stationarity relation with those selected SST indices. The correlations obtained are, however, less significant in general. Lagged correlations between the DJF GCR and the indices of successive 3-month SSTAs averaged over the IPWP and prior to DJF are computed. Results show a robust negative correlation 2 months in advance (Fig. S1a, Online Resource).

This analysis has demonstrated that over the 1925–1970 period, the GCR variability has been mainly driven by tropical SST. Next, the mechanisms associated with IPWP are diagnosed. From the reanalysis data, SSTAs are regressed onto the standardized high-pass SST index of the IPWP over the 1925–1970 period (a time period chosen in the period of stationary linkage between IPWP and GC). Results indicate a global warming of the tropical basins related to a warming of the IPWP. Moreover, this warming is more pronounced in the central and eastern Pacific Ocean, and appears as an El-Niño-like SST pattern (Fig. 9a), which would connect West Africa by the propagation of a Kelvin (Rossby) wave to the East (West) (Rowell 2001; Gill 1980; Matsuno 1966). A warming in the eastern Pacific leads as a result to a rising over the Pacific and a divergence at upper levels. This is illustrated in Fig. 9b, where at 300 hPa, a pair of anticyclones is present over the eastern Pacific, as well as minimum negative potential velocity (Fig. 9c). Over West Africa, the upper-level circulation is characterized by a convergence at 300 hPa, and a subsidence which dries the atmosphere

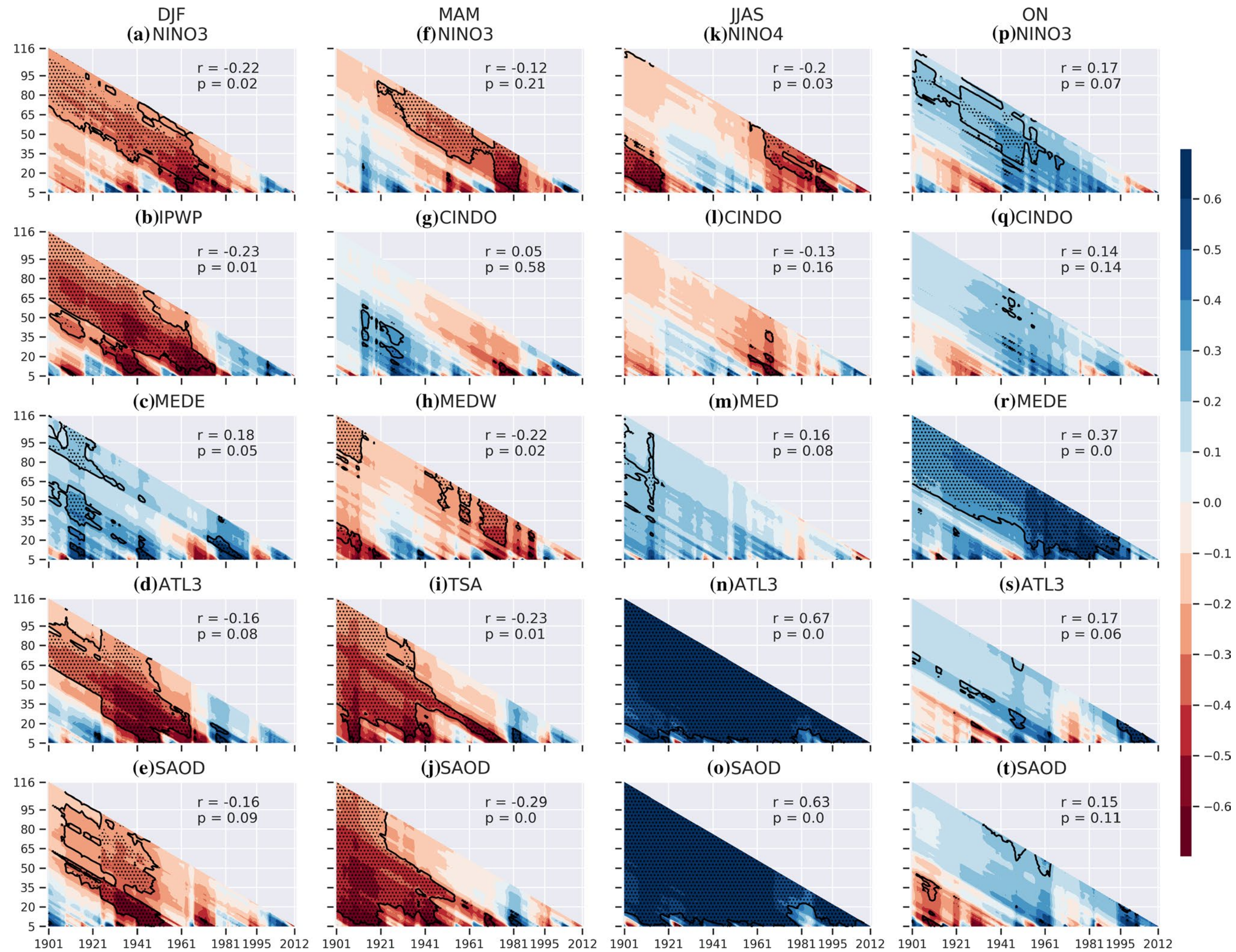

Fig. 7 Running correlation between the interannual component of the Guinean Coast rainfall index and indices of the main SST modes of variability for different starting years (horizontal axis), different window lengths (vertical axis) and different seasons: **a–e** DJF, **f–j** MAM, **k–o** JJAS, **p–t** ON. Contour lines and dots represent significant correlation values at 95% confidence level based on a F test with a standard and effective degree of freedom respectively. Displayed r and p values correspond to the correlation value of the full series and the associated Student-test p_{value} respectively

(Fig. 10a). These conditions stabilize the Guinean Coast atmosphere, thus reducing its rainfall. A similar circulation pattern is obtained when regressing the atmospheric fields onto the Guinean Coast rainfall index (Fig. S10, Online Resource), as it is the case for Niño3 and ATL3 (Fig. S11c, d, Online resource). In the ATL3 positive phases, notherlies converge over the above normal warm sea in the tropical south Atlantic, southward the equator (at around 10° S). Subsequently, the surface winds diverge in Guinea Coast and imply a downward flow which stabilizes the atmosphere.

This analysis has demonstrated that in general, except in the eastern Mediterranean area, the SST changes display a negative correlation with the Guinean Coast rainfall. For some periods, and for long samples, robust linkages are drawn out between several important SST modes of variability and the Guinean Coast rainfall. The results suggest a leading role of the tropical basins in driving the DJF Guinean Coast rainfall, mainly during 1925s–1970s.

4.2 Oceanic forcing of the pre-monsoon (MAM) Guinean Coast rainfall

The pre-monsoon season accounts for 23% of the Guinean Coast annual rainfall (Table 2). Over the 1901–2016 period, the MAM rainfall average ranges between 0 and 3 mm day^{-1} in most of the areas north of 10° N. South of this limit, the mean rainfall rate increases, and fluctuates between 3 and 7 mm day^{-1} (Fig. 4b). The MAM Guinean Coast rainfall mode has a correlation pattern which extends from the coastal areas to the northernmost area of the Sahel (Fig. 4f). The correlation values are overall positives. However, the highest values (between 0.3 and 0.7) are mainly located in

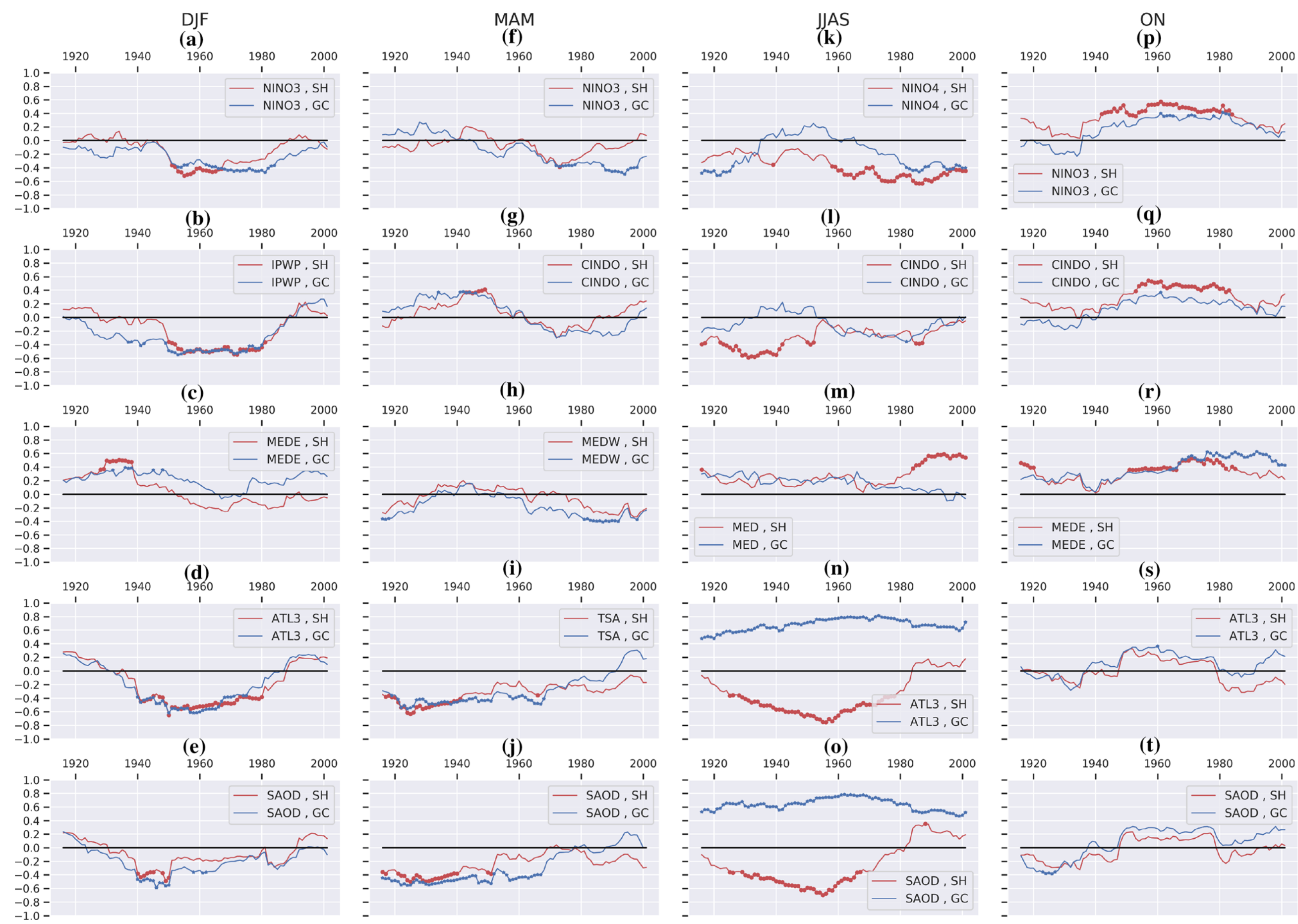

Fig. 8 Running correlation of 31-year sliding window between the Guinean Coast rainfall and SST modes of variability for different seasons (blue curves): **a–e** DJF, **f–j** MAM, **k–o** JJAS, **p–t** ON. Results for the Sahel (red curves) are also shown (but not discussed). Stars and dots mark significant values at 95% confidence level based on a F test with a standard degree of freedom. Years in horizontal axes represent the middle of the 31-year sliding window

the Guinean Coast region. Broadly, compared with the SST pattern obtained in the Harmattan season, the MAM SST anomalies are weakly correlated with the Guinean Coast rainfall index (Fig. 4j). This SST pattern shows significant negative correlations in the tropical South Atlantic, central subtropical South Pacific, and western Mediterranean Sea. In the subtropical South Atlantic and eastern tropical North Pacific, the correlations are positive in very small areas, with similar absolute values.

From Fig. 5, it can be seen that the South Atlantic Ocean Dipole index has the highest correlation with the Guinean Coast rainfall index for the 1901–2016 period (− 0.29), followed by the tropical South Atlantic and the tropical Atlantic SST meridional gradient indices (0.23 and − 0.23 respectively). The results of the correlation between the main SST indices with the Guinean Coast rainfall in MAM are represented in Fig. 6f–j. They suggest that years of warm (cold) phases of the tropical South Atlantic or the South Atlantic Ocean Dipole are associated with a reduction (an intensification) of the West African rainfall. In the coast of Guinea, significant values of the spatial correlation between the TSA and SAOD indices and anomalies of rainfall are mostly restricted to the central southernmost and eastern areas. Finally, the Mediterranean Sea (mainly the western area) also exhibits significant negative correlations in a localized area over to the central coastal regions. The analysis of the robustness of the MAM SST-rainfall interrelation confirms that the South Atlantic Ocean Dipole has the strongest and most stationary link with the Guinean Coast rainfall (Figs. 7j, 8j). For samples starting between 1901 and 1940, and for periods between 20 and 65 years, the correlations calculated range between − 0.4 and − 0.6. In the first 2 decades of the twentieth century, they exceed − 0.6 for shorter samples. Interestingly, this negative correlation is reversed in the 1980s, where a strong coupling has been found between the Niño3 and the Guinean Coast rainfall indices. As a result, after the 1980s, El-Niño positive phases are associated with anomalous cooling in the eastern tropical

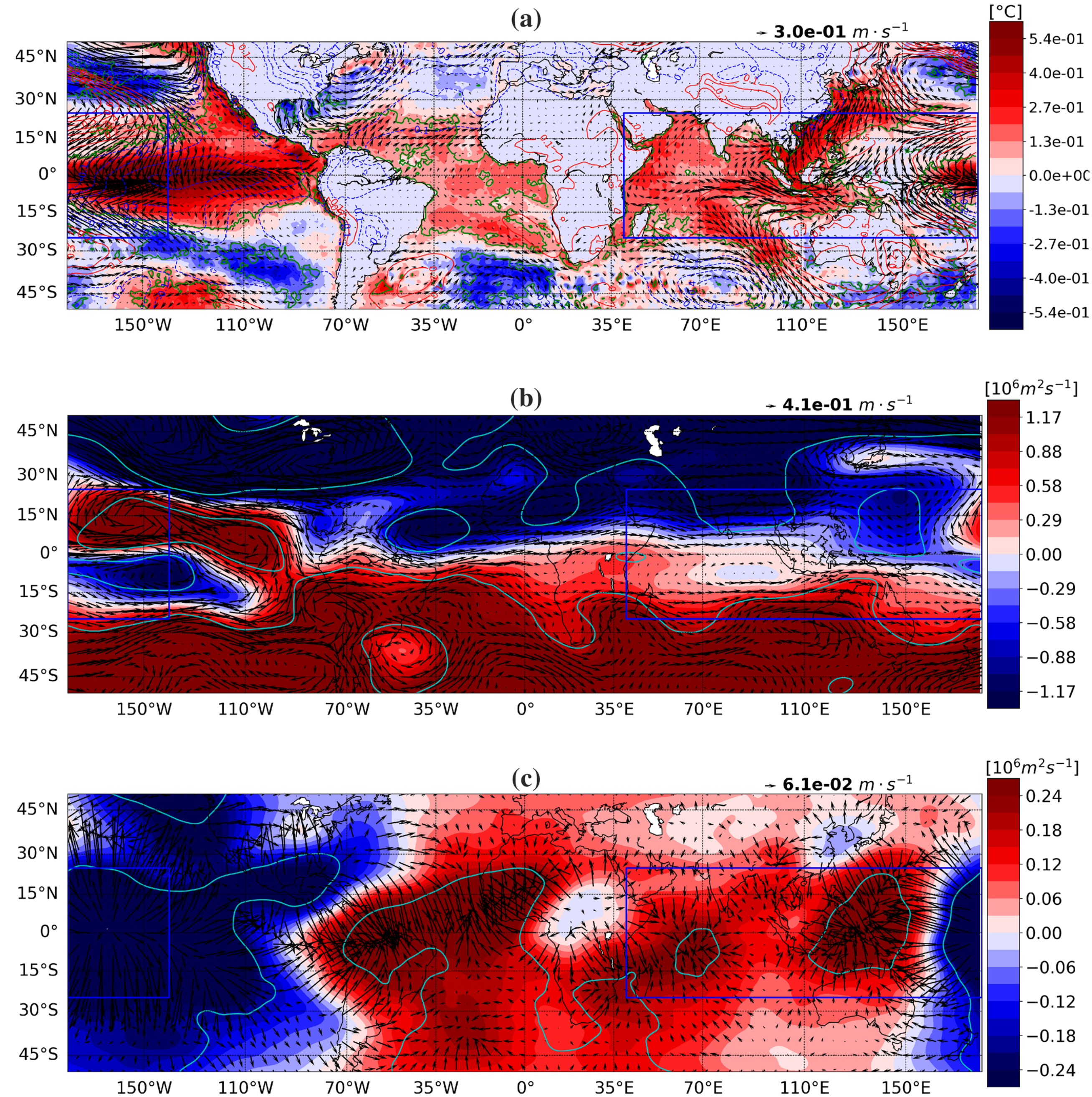

Fig. 9 DJF: regression of **a** sea surface temperature anomalies (colors, in °C), sea level pressure anomalies (blue and red contours, in hPa), surface winds anomalies (arrows); **b** 300 hPa anomalies of streamfunction (colors) and non-divergent component of the wind (arrows); **c** 300 hPa anomalies of potential velocity (colors) and divergent component of the wind (arrows) onto the standardized high-pass IPWP SST index. Green contours in **a**, and blue contours in **b**, **c** indicate significant shaded values at 95% confidence level, according to a Student test. The regressions are computed for the 1925–1970 period. The blue box indicate the area used to compute the Indo-Pacific warm pool SST index

South Atlantic (Fig. S7f, i, j, Online Resource), causing a reduction of rainfall over costal Guinea (Fig. S5f, Online Resource). Thus, the reduction effect of El-Niño should weaken or dominate the rainfall increase related to the cooling of the tropical South Atlantic during this season (Fig. S5i, j, Online Resource). Before the 1980s, the eastern tropical Pacific and the tropical South Atlantic are weakly connected (Fig. S6f, i, Online Resource). Furthermore, the rainfall and SST correlation patterns displayed by indices of the tropical South Atlantic and the South Atlantic Ocean Dipole are similar, as well as their stationarity features. Incidentally, remote effects of SST changes in the western

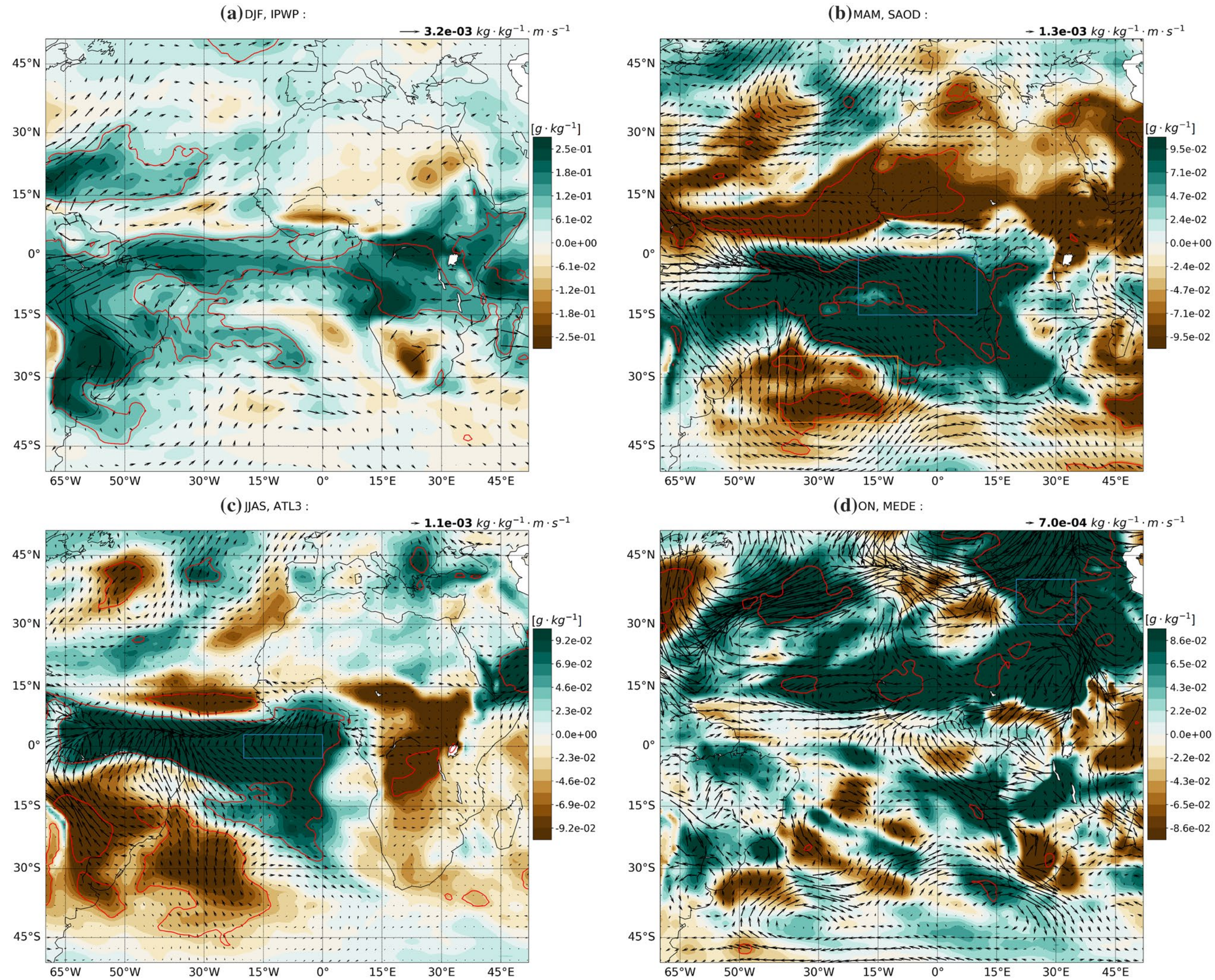

Fig. 10 Regression of anomalies of specific humidity (colors) and moisture flux (arrows) at 850 hPa onto standardized high-pass SST indices of **a** IPWP, **b** SAOD, **c** ATL3, **d** MEDE. Red contours indicate significant specific humidity at 95% confidence level. The blue rectangle on each map delineate the domain used to compute the SST index. The regressions are evaluated for the 1925–1970, 1901–1946, 1901–2010, 1950–1995 periods respectively

Mediterranean Sea on the MAM coastal Guinean rainfall are globally weak and not significant for shorter timescales. Lagged correlations between the GCR in MAM and the successive 3-month means of SST indices indicate that the influence of the tropical South Atlantic and the meridional SST gradient in the tropical Atlantic (TASI, also called the interhemispheric SST mode) starts 2 months in advance, while the delay is 1 month for the South Atlantic Ocean Dipole (Fig. S1b, Online Resource). Further analyses (not shown) demonstrate that the northern and southern core of TASI are not simultaneously coupled between them (which is in accordance with Gu 2010) nor with the Guinean Coast rainfall. As for the SAOD, much of the strong correlations in the stationarity analysis between TASI and GCR coincide with that of the tropical South Atlantic and GCR. This reaveals the importance of the tropical South Atlantic in driving the MAM Guinean Coast rainfall, which could be strengthen by the development of the southern (northern) core of the SAOD (TASI).

From the reanalysis data, the regression map of SSTAs and surface winds associated with the standardized SAOD index (regression over the 1901–1946 period, Fig. S8b, Online Resource) shows that positive phases of the SAOD are associated with warm SST anomalies in the most part of the tropical South Atlantic and cold SSTAs in its south-western area. According to Lindzen–Nigam process (Lindzen and Nigam 1987), these surface gradients of SST anomalies induce anomalous surface pressure gradients which accelerate South-North surface winds from the South West Pole to the North East Pole. In addition, at the equator, winds are northwesterlies. This winds combination produces a surface convergence between 10° S and the equator, followed by an ascent centered at 4° S in the eastern tropical South Atlantic. At upper-levels, the divergent northward wind favors a convergence over West Africa and a subsidence which decreases its humidity (Fig. 10b). In the tropical South Atlantic, positive values of the vertically integrated moisture flux convergence are observed over 0° S–10° S, while they are negative north of the equator, including West Africa (Fig. S9b, Online Resource). The moisture flux divergence in the cost of Guinea is consistent with the subsequent rainfall reduction. Consistently, the circulation fields related to the coastal Guinean rainfall point out a dipole-like pattern of SSTAS in the tropical South Atlantic, and a similar circulation feature (Fig. S12a, b, Online Resource). It also shows in the tropical Atlantic a pattern reminiscent of the interhemispheric mode which is in opposite phase with the SAOD, and increases the cross-equatorial northerlies and their convergence in the north east pole of the SAOD.

The opposite phase relationship between the MAM GCR and the SST anomalies in the tropical South Atlantic is in agreement with the finding of Meynadier et al. (2015), who linked the appearance of a cold tongue in the eastern equatorial Atlantic to the beginning of the early raining season in the coastal regions of West Africa (also Nguyen et al. 2011; Leduc-Leballeur et al. 2012). These cold SST conditions increase the northern front of the cold tongue which accelerates northerlies from the equator to the coast of Guinea. Accordingly, moist air is brought to the Gulf of Guinea and marks the onset of the raining season. Moreover, the appearance of the Atlantic cold tongue has been shown to be related to a strengthening of southeasterlies associated with the northward march of the St Helena anticyclone. It results in an intense upwelling around 4° S (Caniaux et al. 2011).

In summary, except in years around 1980 and afterward, SST changes in the tropical South Atlantic are the main oceanic drivers of the Guinean Coast rainfall variability during the pre-monsoon season. This influence is reinforced by the development of the southern (northern) lobes of the South Atlantic Ocean Dipole (Interhemispheric SST mode). Note that for the selected SST modes, the Sahelian and Guinean Coast rainfall indices have similar covariability stationarity features (Fig. 8f–j).

4.3 Oceanic forcing of the monsoon (JJAS) Guinean Coast rainfall

The JJAS rainfall accounts for 58% of the Guinean Coast annual rainfall (Table 2). Note that the monsoon season in this analysis contains 4 months, unlike the other seasons which have 2 or 3 months. The spatial distribution of the average seasonal rainfall rate reveals highest values (between 7 and 19 mm day^{-1}) in the westernmost (18° W–7° W) and easternmost (4–10° E) areas of the Guinean Coast (Fig. 4c). In the rest of that zone, the rainfall mean values lie between 3 and 7 mm day^{-1}. The rainfall correlation pattern that characterizes the Guinean Coast rainfall variability during this season shows positive values that are positioned in the 5–10° N latitudinal band, stretching from West to East (Fig. 4g). North of 10°N, significant negative weak correlations are obtained in the eastern Sahel. This reveals that the monsoon Guinean Coast rainfall mode is well separated from the Sahelian mode, and this could be explained by differences in external SST forcing of the West African rainfall. For instance, Polo et al. (2008) have analysed the covariability between the boreal summer West African rainfall and the tropical oceanic basins. They showed that the leading mode links the Guinean rainfall mode with the Atlantic Equatorial mode, while the Sahelian rainfall mode is more related to the Mediterranean Sea surface temperature changes. In parallel, the West African Westerly Jet (WAWJ) makes an important contribution to the zonal moisture transport onto the Sahel, as several studies showed a reduction of the rainfall in the Sahel associated with a negative zonal moisture transport, and a weakening of the WAWJ (Lélé et al. 2015). The global-scale SST influence on this jet in summer, could impact its moisture supply to the Sahel, whereas Guinea Coast remains under a more regional SST control.

The Guinean Coast rainfall index correlation with SSTAs in boreal summer highlights two main subregions in the Atlantic Ocean (Fig. 4k). On the one hand, a core of positive correlations appears in the region across the equatorial and southeastern tropical Atlantic. Above (below) normal SST in that region produces positive (negative) Guinean Coast rainfall anomalies. On the other hand, in the southwestern tropical Atlantic, negative correlations are obtained, meaning that below (above) normal SST conditions in that area are associated with an increase (a decrease) in rainfall in the Guinean Coast. Additionally, significant positive correlation values are found in the subtropical North Atlantic, offshore areas in the extratropical North Atlantic and the western tropical Pacific. Weak correlations are seen in the eastern tropical Pacific and Indian Ocean, while negative values are obtained in the Maritime Continent oceanic area and eastward.

The Atlantic Niño and the South Atlantic Ocean Dipole appear as the fundamental oceanic internal modes of variability associated with the boreal summer Guinean Coast rainfall variability. The sign of their correlation is opposite compared with the MAM season. For the 1901–2016 period, both modes have a positive correlation with the Guinean Coast rainfall index, with values of 0.67 and 0.63 for ATL3 and SAOD, respectively (Fig. 5). Figure 6n, o indicate that they tend to create a dipole rainfall pattern in West Africa, with a band of positive correlations in Guinea Coast and negative values in Sahel (Adler et al. 2003; Nnamchi and

Li 2011). Then, warm (cold) phases of the Atlantic Niño or South Atlantic Ocean Dipole are associated with rainfall anomalies of positive (negative) sign in the Guinean Coast and negative (positive) sign in the Sahel. This dipole is present in our analysis because of the long period over which the analysis is performed. It was strong over the 1901–1970 period (Fig. S4n–o, Online Resource), while it weakens afterward (Fig. S5n–o, Online Resource). This is explained by the fact that the global SST in the tropical basins have started to covary with the rainfall in West Africa. After 1970s, positive SST anomalies in the eastern Atlantic equatorial area are indeed associated with negative (positive) SST anomalies in the equatorial eastern Pacific (Maritime Continent oceanic area) , while before 1970s the linkage with the eastern equatorial Pacific is non-existent (Figs. S6 and S7n–o, Online Resource). Thus, as shown by Losada et al. (2012) an increased rainfall over the Sahel associated with those La-Niña conditions cancels the negative rainfall anomaly induced in the Sahel by warm phases of ATL3 (Losada and Rodríguez-Fonseca 2015). Regarding the tropical Pacific, Indian Ocean and the Mediterranean Sea, their influences are more concentrated on the Sahelian area in JJAS over the 1901–2016 period (Fig. 6k–m).

The strong positive correlation between the Guinean Coast rainfall index and both ATL3 and SAOD is stationary over the whole period investigated and at all timescale (Figs. 7n, o, 8n, o). Significant correlation values are generally between 0.5 and 0.8, and exceed 0.8 in several cases. Additionally, the Niño4 and Guinean Coast indices have a non-stationary linkage, with significant negative correlations in the early and last decades of the 1901–2016 period. As for the Indian Ocean, a coupling is found in the 1970s, with negative correlations (Fig. 7i).

Lagged correlations between the JJAS rainfall index of the coast of Guinea and SST indices averaged over the successive 3-month prior to JJAS are displayed in Fig. S1c (Online Resource). Results show a robust negative (positive) correlation with the meridional SST gradient in the tropical Atlantic (tropical South Atlantic) 8 (7) months in advance. Indices of the South Atlantic ocean dipole and Atlantic Niño display the highest correlation (around 0.6) for the first 3 lags and their influence is notable 5 months in advance.

During the monsoon season, ATL3 positive phases lead to a warming of the eastern equatorial Atlantic, which decreases the surface pressure gradient between West Africa and the Atlantic Ocean (Fig. S8c, Online Resource). Trade winds are subsequently weakened, altering the northward penetration of the monsoon flow into West Africa. Moist air converges over the warm water at the equator, rises and is advected to coastal Guinea, as shown in Fig. 10c. The convergence of the moisture flux over the Guinean Coast (Fig. S9c, Online Resource) contributes to increase its rainfall (Giannini 2003; Polo et al. 2008; Rodríguez-Fonseca et al. 2015; Suárez-Moreno et al. 2018). In sum, the JJAS rainfall variability in the Gulf of Guinea is more driven by SST changes in the equatorial and tropical South Atlantic due to the Atlantic Equatorial mode and the South Atlantic Ocean Dipole. A similar circulation feature is obtained when surface and atmospheric fields are regressed onto the Guinean Coast rainfall index (Fig. S12c, d, Online Resource).

4.4 Oceanic forcing of the post-monsoon (ON) Guinean Coast rainfall

The post-monsoon season (October and November) accounts for 15% of the Gulf of Guinea annual rainfall (Table 2). The rainfall mean vary between 1 and 12 mm day^{-1} over the coastal region, with maxima located in its easternmost and westernmost sectors (Fig. 4d). The center of action of the rainfall correlation pattern related to Guinea Coast rainfall mode covers all the West African region, with positive values everywhere. However, correlation maxima stretch across 7° N and 12° N (Fig. 4h). The variability of the Guinean Coast rainfall in ON is in phase with SST changes in the eastern Mediterranean basin, the Red Sea and in very limited tropical South Atlantic areas (Fig. 4i). Overall, the tropical basins are weakly connected with the ON rainfall changes in Guinea Coast.

For the 1901-2016 period, the eastern Mediterranean SST and Guinean Coast rainfall indices present the highest correlation value, 0.37 (Fig. 5). Warm (cold) phases of this oceanic basin cause more (less) rainfall over West Africa, as illustrated in Fig. 6r. During the first half of the twentieth century, the coupling between MEDE and GCR is weak and significant for only long timescales (above 35 years). This connection strengthens from the 1950s, where their correlation values are higher than 0.4 for all timescales above 10 years (Figs. 7r, 8r). During the 1950–1995 period, warm phases of the eastern Mediterranean Sea in ON are associated with a warming of the equatorial and eastern tropical South Atlantic and an increase of the rainfall in the Gulf of Guinea (Fig. S6r, Fig. S4r, s, Online Resource). Nevertheless, prior to the 1950s, SST changes in the eastern Mediterranean Sea are weakly and negatively correlated with SSTAs in the tropical South Atlantic. A warming of the eastern Mediterranean Sea is associated with a cooling of the eastern equatorial Atlantic (Fig. S7r, Online Resource), potentially cancelling their respective effect on the rainfall in the coastal Guinea. As a consequence, the connection between the eastern Mediterranean Sea and the Guinean Coast vanishes over that period. In addition, the correlation between the GCR index and SST anomalies over the 1901–1950 period suggests a strong coupling with SST in the Maritime Continent area, where significant negative values appear. Elsewhere in the tropical basins, the connections are weak, while positive correlations are seen in the eastern Mediterranean basin.

Those changes in the covariability between the different oceanic basin have been shown to produce non-stationarities in the teleconnections processes (Suárez-Moreno et al. 2018).

Furthermore, the Atlantic Equatorial mode displays positive correlations with rainfalls located along the coast of West Africa, while the indices of Niño3 and CINDO show significant positive correlations stretching from the northern limit of the Guinean Coast to Sahel (Fig. 6p, q, s). The influence of ATL3 is noticeable only for shorter timescales over the 1995–2016 period (Fig. 7s). The influence of Niño3 is significant for longer samples (above 35 years) starting before 1970 (Fig. 7p) whereas for shorter samples, no robust link is found.

Several studies show that warm phases of the eastern Mediterranean Sea in summer are associated with a rising of moist air over the basin, which in turn is transported southward by the local wind circulation. This leads to a moisture convergence in the Sahel and Coast of Guinea, with a subsequent increase in rainfall (Fontaine et al. 2009; Gaetani et al. 2010). Regression analysis over the 1950–1995 period during ON reveals that warm situations of the eastern Mediterranean Sea (Fig. S8d, Online Resource) lead to a rising of moist air over the eastern basin, which is then transported by low-level northeasterlies (between 700 and 850 hPa) toward West Africa (Fig. 10d). In addition, moist air from the Atlantic Ocean is brought by the low-level westerlies, southeasterlies and northerlies (in the West flank of the North Africa). Those winds increase the moisture supply to West Africa. Analogously, the regression of the circulation fields onto the Guinean Coast rainfall shows an important warming in the eastern Mediterranean basin (Fig. S13a), and the presence of a cyclonic circulation over northern Africa which transports equatorward moisture by its western flank into West Africa (Fig. S13b,d). A low-level eastward component of the moisture flux is also present in Fig. S13c, resulting in more rainfall over West Africa.

In conclusion, only changes of the eastern Mediterranean SST have a strong and stationary correlation with the interannual Guinean Coast rainfall in the post-monsoon season. Anomalous warming over the Mediterranean Sea strengthens the Saharan Heat Low (SHL) which is in accordance with Diakhaté et al. (2019) hypothesis. Moreover, the maritime extension of the SHL induces over the tropical North Atlantic, a cyclonic circulation that provokes in its southern flank a strong low-level westerly jet (Grodsky 2003; Pu and Cook 2010; Liu et al. 2019) which transports humidity toward the coastal Guinea, leading therefore to an increased rainfall. This mediterranean influence is noticeable 2 months in advance, as shown in Fig. S1d (Online Resource), and is the most robust of the lagged correlations between the SST indices and the ON GCR index. Note that, in this season, the linkages between the Niño3, MEDE and the Guinean Coast rainfall are similar to the one obtained with the Sahelian rainfall. Moreover, Sahelian rainfall linkages with the Indian Ocean and Niño3 are more significant than in the Guinean Coast case (Fig. 8p–r).

5 Conclusion

This study has analyzed the interannual variability of rainfall in the Guinean Coast region and its links with SST changes over the 1901–2016 period. Unlike numerous studies, our analysis is not restricted to the monsoon season (which only accounts for 58% of the annual rainfall in this region) and highlights how the links between rainfall and SST vary according to the season.

Our results show that the JJAS Atlantic influence on the Guinean Coast rainfall is stronger than the impact of all other basins and for all other seasons. The Harmattan (DJF) Guinean Coast rainfall interannual variability has been highly influenced by SST changes in the tropical basins over 1925–1970. Variability of the Indo-Pacific warm pool, El-Niño and Atlantic equatorial mode are anticorrelated with the interannual Guinean Coast rainfall. In DJF, years of larger than average SST in the IPWP are associated with positive SST anomalies in the eastern tropical Pacific. The SST imprint of those conditions appears like an El-Niño event which leads to an eastward/westward propagation of Kelvin/Rossby waves through the atmosphere. This enhances a high level wind convergence over the Guinean Coast, followed by a downward motion of the air column (Rowell 2001), stabilizing the Guinean Coast atmosphere and reducing its rainfall. Moreover, after the 1980s, the connection between the IPWP and the equatorial Atlantic has weakened. This might have reduced the remote effect of IPWP SST changes on the Guinean Coast rainfall.

The pre-monsoon (MAM) and the monsoon (JJAS) rainfall variability of the Guinean Coast are mainly associated with the South Atlantic Ocean Dipole and the Atlantic Niño. Those SST modes are negatively correlated with the pre-monsoon Guinean Coast rainfall, with the strongest impact displayed by the SAOD. Their linkages with the rainfall fluctuations in coastal Guinea are stationary from 1901 to 1980. Afterwards, an inversion of the correlation occurs and is potentially due to the strengthening of the El-Niño remote effect. Contrary to the MAM season, the Atlantic Niño and the South Atlantic Ocean Dipole are both positively correlated with the JJAS Guinean Coast rainfall index. Those SST-rainfall interannual interrelations are stationary over the 1901–2016 period, and stronger than in the previous season. The Atlantic Niño and the Guinean Coast rainfall indices have the highest correlation value for that period. Positive phases of the SAOD and ATL3 modes are associated with negative (positive) Guinean Coast rainfall anomalies in the pre-monsoon

(monsoon) season. Similar physical mechanisms explain the linkages between those Atlantic modes and the Guinean Coast rainfall. In summer, when the SAOD or ATL3 index is above normal, positive SSTAs in the eastern tropical Atlantic lead to a surface winds convergence at the equator and a strong ascent. Moist air is then advected into the Guinean Coast, increasing the rainfall. In the case of a positive phase of the SAOD, the surface wind divergence in the South West Pole strengthens the convergence in the ATL3 area (Nnamchi and Li 2011). In MAM, the surface convergence zone due to the anomalous warming of the tropical South Atlantic in positive phases of the SAOD, is shifted south of the equator. This leads to anomalous subsidence over the coast of Guinea, and a reduction of its rainfall.

The post-monsoon Guinean Coast rainfall regime is more correlated with SST changes in the eastern Mediterranean Sea on interannual timescales. The analysis of their indices shows that they have a positive correlation which is strong and stationary over the 1950–2016 period. The Guinean Coast rainfall increase (decrease) coincides with a zonal incoming (outgoing) low-level moisture flux induced by a strengthening (weakening) of the low level westerly jet in the southern flank of a cyclonic circulation over the tropical North Atlantic, driven in turn by a decrease (increase) of the mean sea level pressure anomalies. This cyclonic circulation over the tropical North Atlantic appears as a maritime extension of the strengthened Saharan Heat Low associated with the anomalous warming in the eastern Mediterranean sea. Interestingly, the robust linkages drawn out provide notable different lagged correlations which are important for the seasonal rainfall forecasting in the coastal Guinea. For DJF, the influence of the IPWP can be predicted 2 months in advance. For the MAM rainfall, the tropical South Atlantic and the meridional SST gradient in the tropical Atlantic present noticeable correlations 2 months in advance. Five months early, the JJAS rainfall is in phase with SST changes in the Atlantic Niño area, while for the ON rainfall, the influence of the eastern Mediterranean Sea can be forecasted 2 months ahead.

Further analyses are still needed to better assess the large-scale oceanic influences on the interannual, decadal to multidecadal variability of the Harmattan, pre-monsoon and post-monsoon rainfalls in the coastal Guinea. It would be particularly valuable to further investigate the time-lagging influence of the oceanic basins, which could be done e.g. via statistical methods like the extended maximum covariance analysis. Finally, our results provide observationally-based diagnostics that could be used for the evaluation of historical simulations performed with climate models. Conversely, SST sensitivity experiments are needed to identify the mechanisms behind those statistical relationships. From this perspective, the Global Monsoons Model Intercomparison (GMMIP) simulations performed in CMIP6 (Zhou et al. 2016) should help address this issue.

Acknowledgements We would like to acknowledge the three reviewers for their constructive comments and suggestions which helped to improve the manuscript. We would also like to thank François Massonnet for commenting on the early version of this work, Alina Gainusa-Bogdan and Andreas Fink for their useful remarks. We acknowledge the European Center for Medium-Range Weather Forecasts which provide the ERA-20C reanalysis data. We finally thank the Met Office Hadley Centre and the Climatic Research Unit for providing the observational data used in this work.

Compliance with ethical standards

Conflict of interest We wish to confirm that there are no known conflicts of interest associated with this publication and there has been no significant financial support for this work that could have influenced its outcome. We confirm that the manuscript has been read and approved by all named authors and that there are no other persons who satisfied the criteria for authorship but are not listed. The manuscript has not been published previously and is not under consideration for publication elsewhere. We confirm that we have given due consideration to the protection of intellectual property associated with this work and that there are no impediments to publication, including the timing of publication, with respect to intellectual property. In so doing we confirm that we have followed the regulations of our institutions concerning intellectual property. We understand that the Corresponding Author (Koffi Worou) is the sole contact for the Editorial process (including Editorial Manager and direct communications with the office). He is responsible for communicating with the other authors about progress, submissions of revisions and final approval of proofs. We confirm that we have provided a current, correct email address which is accessible by the corresponding author and which has been configured to accept email from koffi.worou@uclouvain.be.

References

Abiodun BJ, Adeyewa ZD, Oguntunde PG, Salami AT, Ajayi VO (2012) Modeling the impacts of reforestation on future climate in west africa. Theor Appl Climatol 110(1–2):77–96. https://doi.org/10.1007/s00704-012-0614-1

Adejuwon JO, Odekunle TO (2006) Variability and the severity of the "little dry season" in southwestern nigeria. J Clim 19(3):483–493. https://doi.org/10.1175/jcli3642.1

Adler RF, Huffman GJ, Chang A, Ferraro R, Xie PP, Janowiak J, Rudolf B, Schneider U, Curtis S, Bolvin D, Gruber A, Susskind J, Arkin P, Nelkin E (2003) The version-2 global precipitation climatology project (GPCP) monthly precipitation analysis (1979-present). J Hydrometeorol 4(6):1147–1167. https://doi.org/10.1175/1525-7541(2003)004<1147:tvgpcp>2.0.co;2

Bader J, Latif M (2003) The impact of decadal-scale Indian ocean sea surface temperature anomalies on Sahelian rainfall and the north Atlantic Oscillation. Geophys Res Lett. https://doi.org/10.1029/2003gl018426

Bamba A, Dieppois B, Konaré A, Pellarin T, Balogun A, Dessay N, Kamagaté B, Savané I, Diédhiou A (2015) Changes in vegetation and rainfall over west africa during the last three decades (1981–2010). Atmos Clim Sci 05(04):367–379. https://doi.org/10.4236/acs.2015.54028

Berntell E, Zhang Q, Chafik L, Körnich H (2018) Representation of multidecadal Sahel rainfall variability in 20th century reanalyses. Sci Rep. https://doi.org/10.1038/s41598-018-29217-9

Dian B (1978) Aspects géographiques du binôme café cacao dans l'économie ivoirienne. Nouvelles Editions africaines, Abidjan-Dakar

Brou Y, NGoran J, Bicot S, Servat E (2003) Risque climatique et production agricole en côte d'ivoire: effet des variations pluviométriques sur la production cacaoyère. In: Actes de la 14ème conférence internationale sur la recherche cacaoyère

Caniaux G, Giordani H, Redelsperger JL, Guichard F, Key E, Wade M (2011) Coupling between the Atlantic cold tongue and the west african monsoon in boreal spring and summer. J Geophys Res. https://doi.org/10.1029/2010jc006570

Cook KH (1999) Generation of the African easterly jet and its role in determining west African precipitation. J Clim 12(5):1165–1184. https://doi.org/10.1175/1520-0442(1999)012<1165:gotaej>2.0.co;2

Deckker PD (2016) The indo-pacific warm pool: critical to world oceanography and world climate. Geosci Lett. https://doi.org/10.1186/s40562-016-0054-3

Dettwiller J (1965) Note sur la structure du front intertropical boréal sur le nord-ouest de l'afrique. Meteorologie 6:337–347

Diakhaté M, Rodríguez-Fonseca B, Gómara I, Mohino E, Dieng AL, Gaye AT (2019) Oceanic forcing on interannual variability of Sahel heavy and moderate daily rainfall. J Hydrometeorol 20(3):397–410. https://doi.org/10.1175/jhm-d-18-0035.1

Diatta S, Fink AH (2014) Statistical relationship between remote climate indices and west african monsoon variability. Int J Climatol 34(12):3348–3367. https://doi.org/10.1002/joc.3912

Dommenget D, Latif M (2000) Interannual to decadal variability in the tropical Atlantic. J Clim 13(4):777–792. https://doi.org/10.1175/1520-0442(2000)013<0777:itdvit>2.0.co;2

Dommenget D, Latif M (2002) A cautionary note on the interpretation of EOFs. J Clim 15(2):216–225. https://doi.org/10.1175/1520-0442(2002)015<0216:acnoti>2.0.co;2

Duchon CE (1979) Lanczos filtering in one and two dimensions. J Appl Meteorol 18(8):1016–1022. https://doi.org/10.1175/1520-0450(1979)018<1016:lfioat>2.0.co;2

Ehounou JN, Kouamé B, Tahi MG, Kassin EK, Dékoula CS, Yao GF, Kouadio HK, N'guessan AEB, Soro N (2019a) Impact of local global warming on rainfall and annual cocoa water requirements in the regions of lôh-djiboua and gôh in west-central côte d'ivoire. Int J Environ Clim Change. https://doi.org/10.9734/ijecc/2019/v9i930135

Ehounou JN, Kouamé B, Tahi MG, Kassin EK, Kotaix JAA, Dékoula CS, Yao GF, Kouadio HK, N'guessan AEB, Soro N (2019b) Global warming influence on major seasonal and intra-seasonal rainfall indicators for sustainable cocoa production in west-central côte d'ivoire. J Exp Agric Int. https://doi.org/10.9734/jeai/2019/v40i530378

Fink AH, Engel T, Ermert V, van der Linden R, Schneidewind M, Redl R, Afiesimama E, Thiaw WM, Yorke C, Evans M, Janicot S (2017) Mean climate and seasonal cycle. In: Parker DJ, Diop-Kane M (eds) Meteorology of tropical West Africa: the forecasters' hand-book. Wiley, pp 1–39. https://doi.org/10.1002/9781118391297.ch1

Fink A, Speth P (1997) Some potential forcing mechanisms of the year-to-year variability of the tropical convection and its intraseasonal (25–70-day) variability. Int J Climatol 17(14):1513–1534. https://doi.org/10.1002/(SICI)1097-0088(19971130)17:14<1513::AID-JOC210>3.0.CO;2-U

Folland CK, Palmer TN, Parker DE (1986) Sahel rainfall and worldwide sea temperatures, 1901–85. Nature 320(6063):602–607. https://doi.org/10.1038/320602a0

Fontaine B, Garcia-Serrano J, Roucou P, Rodriguez-Fonseca B, Losada T, Chauvin F, Gervois S, Sijikumar S, Ruti P, Janicot S (2009) Impacts of warm and cold situations in the Mediterranean basins on the west african monsoon: observed connection patterns (1979–2006) and climate simulations. Clim Dyn 35(1):95–114. https://doi.org/10.1007/s00382-009-0599-3

Froidurot S, Diedhiou A (2017) Characteristics of wet and dry spells in the west african monsoon system. Atmos Sci Lett 18(3):125–131. https://doi.org/10.1002/asl.734

Gaetani M, Fontaine B, Roucou P, Baldi M (2010) Influence of the mediterranean sea on the west african monsoon: Intraseasonal variability in numerical simulations. J Geophys Res Atmos. https://doi.org/10.1029/2010jd014436

García-Serrano J, Losada T, Rodríguez-Fonseca B, Polo I (2008) Tropical Atlantic variability modes (1979–2002). part II: time-evolving atmospheric circulation related to SST-forced tropical convection. J Clim 21(24):6476–6497. https://doi.org/10.1175/2008jcli2191.1

Germain H (1968) Météorologie dynamique et climatologie; application au régime des pluies au sénégal. ASECNA,Direction de l'Exploitation Météorologique, Dakar, Senegal

Giannini A (2003) Oceanic forcing of Sahel rainfall on interannual to interdecadal time scales. Science 302(5647):1027–1030. https://doi.org/10.1126/science.1089357

Gill AE (1980) Some simple solutions for heat-induced tropical circulation. Q J R Meteorol Soc 106(449):447–462. https://doi.org/10.1002/qj.49710644905

Gómara I, Mohino E, Losada T, Domínguez M, Suárez-Moreno R, Rodríguez-Fonseca B (2017) Impact of dynamical regionalization on precipitation biases and teleconnections over west africa. Clim Dyn 50(11–12):4481–4506. https://doi.org/10.1007/s00382-017-3886-4

Grodsky SA (2003) Near surface westerly wind jet in the Atlantic ITCZ. Geophys Res Lett. https://doi.org/10.1029/2003gl017867

Gu G (2010) Summer-time rainfall variability in the tropical Atlantic. In: Simard S (ed) Climate change and variability. Sciyo, pp 45–66. https://doi.org/10.5772/1743

Gu G, Adler RF (2004) Seasonal evolution and variability associated with the west African monsoon system. J Clim 17(17):3364–3377. https://doi.org/10.1175/1520-0442(2004)017<3364:seavaw>2.0.co;2

Hagos S, Zhang C (2009) Diabatic heating, divergent circulation and moisture transport in the african monsoon system. Q J R Meteorol Soc 136(S1):411–425. https://doi.org/10.1002/qj.538

Hamilton RA, Archbold JW, Douglas CKM (1945) Meteorology of nigeria and adjacent territory. Q J R Meteorol Soc 71(309–310):231–264. https://doi.org/10.1002/qj.49707130905

Harris I, Jones P, Osborn T, Lister D (2013) Updated high-resolution grids of monthly climatic observations—the CRU TS3.10 dataset. Int J Climatol 34(3):623–642. https://doi.org/10.1002/joc.3711

Hirahara S, Ishii M, Fukuda Y (2014) Centennial-scale sea surface temperature analysis and its uncertainty. J Clim 27(1):57–75. https://doi.org/10.1175/jcli-d-12-00837.1

Hsieh JS, Cook KH (2005) Generation of african easterly wave disturbances: relationship to the african easterly jet. Mon Weather Rev 133(5):1311–1327. https://doi.org/10.1175/mwr2916.1

Huang B, Thorne PW, Smith TM, Liu W, Lawrimore J, Banzon VF, Zhang HM, Peterson TC, Menne M (2016) Further exploring and quantifying uncertainties for extended reconstructed sea surface temperature (ERSST) version 4 (v4). J Clim 29(9):3119–3142. https://doi.org/10.1175/jcli-d-15-0430.1

Hulme M (1992) Rainfall changes in Africa: 1931–1960 to 1961–1990. Int J Climatol 12(7):685–699. https://doi.org/10.1002/joc.3370120703

Janicot S, Lafore JP, Thorncroft C (2011) The west African monsoon. In: Chih-Pei C, Yihui D, Ngar-Cheung L, Richard HJ, Bin W, Tetsuzo Y (eds) The global monsoon system: research and forecast, 2nd edn. World Scientific, pp 111–135. https://doi.org/10.1142/9789814343411_0008

Jung T, Ferranti L, Tompkins AM (2006) Response to the summer of 2003 Mediterranean SST anomalies over Europe and Africa. J Clim 19(20):5439–5454. https://doi.org/10.1175/jcli3916.1

Kassin KE, Doffangui K, Kouamé B, Yoro RG, Assa A (2008) Variabilité pluviométrique et perspectives pour la replantation cacaoyère dans le centre ouest de la côte d'ivoire. J Appl Biosci 12:633–641

Kebe I, Sylla MB, Omotosho JA, Nikiema PM, Gibba P, Giorgi F (2016) Impact of GCM boundary forcing on regional climate modeling of west African summer monsoon precipitation and circulation features. Clim Dyn 48(5–6):1503–1516. https://doi.org/10.1007/s00382-016-3156-x

Keenlyside NS, Latif M (2007) Understanding equatorial Atlantic interannual variability. J Clim 20(1):131–142. https://doi.org/10.1175/jcli3992.1

Knight JR, Folland CK, Scaife AA (2006) Climate impacts of the Atlantic multidecadal oscillation. Geophys Res Lett. https://doi.org/10.1029/2006gl026242

Köhler M, Schwendenmann L, Hölscher D (2010) Throughfall reduction in a cacao agroforest: tree water use and soil water budgeting. Agric For Meteorol 150(7–8):1079–1089. https://doi.org/10.1016/j.agrformet.2010.04.005

Kucharski F, Joshi MK (2017) Influence of tropical south Atlantic sea-surface temperatures on the Indian summer monsoon in CMIP5 models. Q J R Meteorol Soc 143(704):1351–1363. https://doi.org/10.1002/qj.3009

Lachenaud P (1991) Facteurs de la fructification chez les cacaoyers (*Theobroma cacao* L.). influence sur le nombre de graines par fruit. Ph.D. thesis

Lachenaud P (1987) L'association cacaoyer-bananier plantain. Etude de dispositifs. Café Cacao Thé 31(3):195–202

Lahive F, Hadley P, Daymond AJ (2018) The physiological responses of cacao to the environment and the implications for climate change resilience. A review. Agron Sustain Dev. https://doi.org/10.1007/s13593-018-0552-0

Lavaysse C, Flamant C, Evan A, Janicot S, Gaetani M (2015) Recent climatological trend of the saharan heat low and its impact on the west African climate. Clim Dyn 47(11):3479–3498. https://doi.org/10.1007/s00382-015-2847-z

Leduc-Leballeur M, de Coëtlogon G, Eymard L (2012) Air–sea interaction in the gulf of guinea at intraseasonal time-scales: wind bursts and coastal precipitation in boreal spring. Q J R Meteorol Soc 139(671):387–400. https://doi.org/10.1002/qj.1981

Lélé MI, Leslie LM (2016) Intraseasonal variability of low-level moisture transport over west africa. Clim Dyn 47(11):3575–3591. https://doi.org/10.1007/s00382-016-3334-x

Lélé MI, Leslie LM, Lamb PJ (2015) Analysis of low-level atmospheric moisture transport associated with the west African monsoon. J Clim 28(11):4414–4430. https://doi.org/10.1175/jcli-d-14-00746.1

Li G, Ren B, Yang C, Zheng J (2010) Indices of el niño and el niño modoki: an improved el niño modoki index. Adv Atmos Sci 27(5):1210–1220. https://doi.org/10.1007/s00376-010-9173-5

Lindzen RS, Nigam S (1987) On the role of sea surface temperature gradients in forcing low-level winds and convergence in the tropics. J Atmos Sci 44(17):2418–2436. https://doi.org/10.1175/1520-0469(1987)044<2418:otross>2.0.co;2

Liu W, Cook KH, Vizy EK (2019) Role of the west african westerly jet in the seasonal and diurnal cycles of precipitation over west Africa. Clim Dyn 54(1–2):843–861. https://doi.org/10.1007/s00382-019-05035-1

Losada T, Rodríguez-Fonseca B (2015) Tropical atmospheric response to decadal changes in the Atlantic equatorial mode. Clim Dyn 47(3–4):1211–1224. https://doi.org/10.1007/s00382-015-2897-2

Losada T, Rodríguez-Fonseca B, Polo I, Janicot S, Gervois S, Chauvin F, Ruti P (2009) Tropical response to the Atlantic equatorial mode: AGCM multimodel approach. Clim Dyn 35(1):45–52. https://doi.org/10.1007/s00382-009-0624-6

Losada T, Rodríguez-Fonseca B, Janicot S, Gervois S, Chauvin F, Ruti P (2010) A multi-model approach to the Atlantic equatorial mode: impact on the west African monsoon. Clim Dyn 35(1):29–43. https://doi.org/10.1007/s00382-009-0625-5

Losada T, Rodriguez-Fonseca B, Mohino E, Bader J, Janicot S, Mechoso CR (2012) Tropical SST and Sahel rainfall: a non-stationary relationship. Geophys Res Lett. https://doi.org/10.1029/2012gl052423

Martin ER, Thorncroft CD (2014) The impact of the amo on the west African monsoon annual cycle. Q J R Meteorol Soc 140(678):31–46. https://doi.org/10.1002/qj.2107

Matsuno T (1966) Quasi-geostrophic motions in the equatorial area. J Meteorol Soc Jpn Ser II 44(1):25–43. https://doi.org/10.2151/jmsj1965.44.1_25

Meynadier R, de Coëtlogon G, Leduc-Leballeur M, Eymard L, Janicot S (2015) Seasonal influence of the sea surface temperature on the low atmospheric circulation and precipitation in the eastern equatorial Atlantic. Clim Dyn 47(3–4):1127–1142. https://doi.org/10.1007/s00382-015-2892-7

Mohino E, Losada T (2015) Impacts of the Atlantic equatorial mode in a warmer climate. Clim Dyn 45(7):2255–2271. https://doi.org/10.1007/s00382-015-2471-y

Mohino E, Janicot S, Bader J (2011a) Sahel rainfall and decadal to multi-decadal sea surface temperature variability. Clim Dyn 37(3):419–440. https://doi.org/10.1007/s00382-010-0867-2

Mohino E, Rodríguez-Fonseca B, Mechoso CR, Gervois S, Ruti P, Chauvin F (2011b) Impacts of the tropical Pacific/Indian oceans on the seasonal cycle of the west African monsoon. J Clim 24(15):3878–3891. https://doi.org/10.1175/2011jcli3988.1

Monahan AH, Fyfe JC, Ambaum MHP, Stephenson DB, North GR (2009) Empirical orthogonal functions: the medium is the message. J Clim 22(24):6501–6514. https://doi.org/10.1175/2009jcli3062.1

Nguyen H, Thorncroft CD, Zhang C (2011) Guinean Coastal rainfall of the west african monsoon. Q J R Meteorol Soc 137(660):1828–1840. https://doi.org/10.1002/qj.867

Nicholson SE (2009) A revised picture of the structure of the "monsoon" and land ITCZ over west Africa. Clim Dyn 32(7–8):1155–1171. https://doi.org/10.1007/s00382-008-0514-3

Nicholson SE (2013) The west African Sahel: a review of recent studies on the rainfall regime and its interannual variability. ISRN Meteorol 2013:1–32. https://doi.org/10.1155/2013/453521

Nicholson SE, Grist JP (2003) The seasonal evolution of the atmospheric circulation over west africa and equatorial Africa. J Clim 16(7):1013–1030. https://doi.org/10.1175/1520-0442(2003)016<1013:tseota>2.0.co;2

Nnamchi HC, Li J (2011) Influence of the south Atlantic ocean dipole on west african summer precipitation. J Clim 24(4):1184–1197. https://doi.org/10.1175/2010JCLI3668.1

Okoro UK, Chen W, Nath D, Nnamchi HC (2019) Variability and trends of atmospheric moisture in recent west African monsoon season and the coordinated regional downscaling experiment-africa projected 21st century scenarios. Int J Climatol 40(2):1149–1163. https://doi.org/10.1002/joc.6261

Park J, Bader J, Matei D (2016) Anthropogenic mediterranean warming essential driver for present and future Sahel rainfall. Nat Clim Change 6(10):941–945. https://doi.org/10.1038/nclimate3065

Poli P, Hersbach H, Dee DP, Berrisford P, Simmons AJ, Vitart F, Laloyaux P, Tan DGH, Peubey C, Thépaut JN, Trémolet Y, Hólm

EV, Bonavita M, Isaksen L, Fisher M (2016) ERA-20c: an atmospheric reanalysis of the twentieth century. J Clim 29(11):4083–4097. https://doi.org/10.1175/jcli-d-15-0556.1

Polo I, Rodríguez-Fonseca B, Losada T, García-Serrano J (2008) Tropical Atlantic variability modes (1979–2002). Part i: time-evolving sst modes related to west African rainfall. J Clim 21(24):6457–6475. https://doi.org/10.1175/2008JCLI2607.1

Pu B, Cook KH (2010) Dynamics of the west African westerly jet. J Clim 23(23):6263–6276. https://doi.org/10.1175/2010jcli3648.1

Rayner NA (2003) Global analyses of sea surface temperature, sea ice, and night marine air temperature since the late nineteenth century. J Geophys Res. https://doi.org/10.1029/2002jd002670

Richter I, Behera SK, Masumoto Y, Taguchi B, Sasaki H, Yamagata T (2012) Multiple causes of interannual sea surface temperature variability in the equatorial Atlantic ocean. Nat Geosci 6(1):43–47. https://doi.org/10.1038/ngeo1660

Rodríguez-Fonseca B, Janicot S, Mohino E, Losada T, Bader J, Caminade C, Chauvin F, Fontaine B, García-Serrano J, Gervois S, Joly M, Polo I, Ruti P, Roucou P, Voldoire A (2011) Interannual and decadal sst-forced responses of the west African monsoon. Atmos Sci Lett 12(1):67–74. https://doi.org/10.1002/asl.308

Rodríguez-Fonseca B, Mohino E, Mechoso CR, Caminade C, Biasutti M, Gaetani M, Garcia-Serrano J, Vizy EK, Cook K, Xue Y, Polo I, Losada T, Druyan L, Fontaine B, Bader J, Doblas-Reyes FJ, Goddard L, Janicot S, Arribas A, Lau W, Colman A, Vellinga M, Rowell DP, Kucharski F, Voldoire A (2015) Variability and predictability of west african droughts: a review on the role of sea surface temperature anomalies. J Clim 28(10):4034–4060. https://doi.org/10.1175/JCLI-D-14-00130.1

Rowell DP (2001) Teleconnections between the tropical pacific and the Sahel. Q J R Meteorol Soc 127(575):1683–1706. https://doi.org/10.1002/qj.49712757512

Rowell DP (2003) The impact of Mediterranean SSTs on the Sahelian rainfall season. J Clim 16(5):849–862. https://doi.org/10.1175/1520-0442(2003)016<0849:tiomso>2.0.co;2

Rowell DP (2013) Simulating SST teleconnections to africa: what is the state of the art? J Clim 26(15):5397–5418. https://doi.org/10.1175/jcli-d-12-00761.1

Saj S, Jagoret P, Etoa LE, Fonkeng EE, Tarla JN, Nieboukaho JDE, Sakouma KM (2017) Lessons learned from the long-term analysis of cacao yield and stand structure in central cameroonian agroforestry systems. Agric Syst 156:95–104. https://doi.org/10.1016/j.agsy.2017.06.002

Salih AA, Elagib NA, Tjernström M, Zhang Q (2018) Characterization of the Sahelian-sudan rainfall based on observations and regional climate models. Atmos Res 202:205–218. https://doi.org/10.1016/j.atmosres.2017.12.001

Sansom HW (1965) The structure and behavior of the inter-tropical convergence zone (ITCZ). In: WMO Technical Note, No 69, pp 91–108, Geneva

Schubert SD, Stewart RE, Wang H, Barlow M, Berbery EH, Cai W, Hoerling MP, Kanikicharla KK, Koster RD, Lyon B, Mariotti A, Mechoso CR, Müller OV, Rodriguez-Fonseca B, Seager R, Seneviratne SI, Zhang L, Zhou T (2016) Global meteorological drought: a synthesis of current understanding with a focus on sst drivers of precipitation deficits. J Clim 29(11):3989–4019. https://doi.org/10.1175/JCLI-D-15-0452.1

Senghor H, Machu É, Hourdin F, Gaye AT (2017) Seasonal cycle of desert aerosols in western africa: analysis of the coastal transition with passive and active sensors. Atmos Chem Phys 17(13):8395–8410. https://doi.org/10.5194/acp-17-8395-2017

Shekhar R, Boos WR (2017) Weakening and shifting of the saharan shallow meridional circulation during wet years of the west African monsoon. J Clim 30(18):7399–7422. https://doi.org/10.1175/jcli-d-16-0696.1

Steinig S, Harlaß J, Park W, Latif M (2018) Sahel rainfall strength and onset improvements due to more realistic Atlantic cold tongue development in a climate model. Sci Rep. https://doi.org/10.1038/s41598-018-20904-1

Suárez-Moreno R, Rodríguez-Fonseca B, Barroso JA, Fink AH (2018) Interdecadal changes in the leading ocean forcing of Sahelian rainfall interannual variability: atmospheric dynamics and role of multidecadal SST background. J Clim 31(17):6687–6710. https://doi.org/10.1175/jcli-d-17-0367.1

Sylla MB, Giorgi F, Ruti PM, Calmanti S, Dell'Aquila A (2011) The impact of deep convection on the west African summer monsoon climate: a regional climate model sensitivity study. Q J R Meteorol Soc 137(659):1417–1430. https://doi.org/10.1002/qj.853

Taubenheim J (1969) Statistische Auswertung geophysikalischer und meteorologischer Daten, vol 5. Akademische Verlagsgesellschaft Geest & Portig

Taubenheim J (1974) Zur berucksichtigung der autokorrelation bei der statistischen signifikanzprufung von korrelation zwischen zwei zeitreihen. Gerlands Beitrage zur Geophysik 83:413–415

Thorncroft CD, Blackburn M (1999) Maintenance of the African easterly jet. Q J R Meteorol Soc 125(555):763–786. https://doi.org/10.1002/qj.49712555502

Thorncroft CD, Hoskins BJ (1994a) An idealized study of African easterly waves. I: a linear view. Q J R Meteorol Soc 120(518):953–982. https://doi.org/10.1002/qj.49712051809

Thorncroft CD, Hoskins BJ (1994b) An idealized study of african easterly waves. II: a nonlinear view. Q J R Meteorol Soc 120(518):983–1015. https://doi.org/10.1002/qj.49712051810

Tokinaga H, Xie SP (2011) Weakening of the equatorial Atlantic cold tongue over the past 6 decades. Nat Geosci 4(4):222–226. https://doi.org/10.1038/ngeo1078

United Nations, Department of Economic and Social Affairs, Population Division (2019) World Population Prospects 2019, volume I: comprehensive Tables (ST/ESA/SER.A/426). United Nations. https://population.un.org/wpp/Publications/Files/WPP2019_Volume-I_Comprehensive-Tables.pdf. Accessed 17 June 2019

University of East Anglia Climatic Research Unit (CRU), Harris IC, Jones PD (2017) Cru ts4.01: climatic research unit (cru) time-series (ts) version 4.01 of high-resolution gridded data of month-by-month variation in climate (Jan. 1901–Dec. 2016). https://doi.org/10.5285/58a8802721c94c66ae45c3baa4d814d0

Villamayor J, Mohino E, Khodri M, Mignot J, Janicot S (2018) Atlantic control of the late nineteenth-century Sahel humid period. J Clim 31(20):8225–8240. https://doi.org/10.1175/jcli-d-18-0148.1

Walker H (1957) Weather and climate of Ghana. Department Note 5, Ghana Meteorological Department

Weller E, Min SK, Cai W, Zwiers FW, Kim YH, Lee D (2016) Human-caused indo-pacific warm pool expansion. Sci Adv 2(7):e1501719. https://doi.org/10.1126/sciadv.1501719

Wilks D (2011) Principal component (EOF) analysis. In: Statistical methods in the atmospheric sciences. International Geophysics, 3rd edn. Elsevier, pp 519–562. https://doi.org/10.1016/b978-0-12-385022-5.00012-9

Zhang C, Woodworth P, Gu G (2006) The seasonal cycle in the lower troposphere over west Africa from sounding observations. Q J R Meteorol Soc 132(621):2559–2582. https://doi.org/10.1256/qj.06.23

Zhou T, Turner AG, Kinter JL, Wang B, Qian Y, Chen X, Wu B, Wang B, Liu B, Zou L, He B (2016) GMMIP (v1.0) contribution to CMIP6: global monsoons model inter-comparison project. Geosci Model Dev 9(10):3589–3604. https://doi.org/10.5194/gmd-9-3589-2016